Inorg. Chem. **2008**, *47*, 1925−1939

Mixed-Valence Tetra- and Hexanuclear Manganese Complexes from the Flexibility of Pyridine-Containing β-Diketone Ligands

Chen-I Yang,[†] Wolfgang Wernsdorfer,[‡] Yu-Jhe Tsai,[†] George Chung,[†] Ting-Shen Kuo,[||] Gene-Hsiang Lee,[§] Minghuey Shieh,[||] and Hui-Lien Tsai*[,†]

Department of Chemistry, National Cheng Kung University, Tainan, 701, Taiwan, Republic of China, Laboratoire Louis Néel, Centre National de la Recherche Scientifique (CNRS), BP-166, 38042 Grenoble Cedex 9, France, Department of Chemistry, National Taiwan Normal University, Taipei 116, Taiwan, Republic of China, and Instrumentation Center, College of Science, National Taiwan University, Taipei, 106, Taiwan, Republic of China

Received July 6, 2007

The reactions of $[Mn_3O(O_2CCCl_3)_6(H_2O)_3]$ with 1-phenyl-3-(2-pyridyl)propane-1,3-dione (HL^1) and 1-(2-pyridly)-3-(*p*-tolyl)propane-1,3-dione (HL^2) in CH_2Cl_2 afford the mixed-valence $Mn^{II}_2Mn^{III}_2$ tetranuclear complexes $[Mn_4O(O_2CCCl_3)_6(L^1)_2]$ (**1**) and $[Mn_4O(O_2CCCl_3)_6L_2^2]$ (**2**), respectively. Similar reactions employing $[Mn_3O(O_2CPh)_6(H_2O)(py)_2]$ with HL^1 and HL^2 give the $Mn^{II}_3Mn^{III}_3$ hexanuclear complexes $[Mn_6O_2(O_2CPh)_8(L^1)_3]$ (**3**) and $[Mn_6O_2(O_2CPh)_8L_3^2]$ (**4**), respectively. Complexes $\mathbf{1}\cdot 2CH_2Cl_2$, $\mathbf{2}\cdot 2CH_2Cl_2\cdot H_2O$, $\mathbf{3}\cdot 1.5CH_2Cl_2\cdot Et_2O\cdot H_2O$, and $\mathbf{4}\cdot 2CH_2Cl_2$ crystallize in the triclinic space group $P\bar{1}$, monoclinic space group $P2_1/c$, monoclinic space group $P2_1/n$, and monoclinic space group $P2_1/n$, respectively. Complexes **1** and **2** consist of a trapped-valence tetranuclear core of $[Mn^{II}_2Mn^{III}_2(\mu_4\text{-}O)]^{8+}$, and complexes **3** and **4** represent a new structural type, possessing a $[Mn^{II}_3Mn^{III}_3(\mu_4\text{-}O)_2]^{11+}$ core. The magnetic data indicate that complexes **3** and **4** have a ground-state spin value of $S = {}^7/_2$ with significant magnetoanisotropy as gauged by the *D* values of -0.51 cm^{-1} and -0.46 cm^{-1}, respectively, and frequency-dependent out-of-phase signals in alternating current magnetic susceptibility studies indicate their superparamagnetic behavior. In contrast, complexes **1** and **2** are low-spin molecules with an $S = 1$ ground state. Single-molecule magnetism behavior confirmed for **3** the presence of sweep-rate and temperature-dependent hysteresis loops in single-crystal *M* versus *H* studies at temperatures down to 40 mK.

Introduction

Polynuclear manganese oxide clusters have attracted interest for two main reasons. First, from the biological point of view, there has been considerable interest in understanding the structures and properties of the synthetic models for mimicking the active site of metalloenzymes containing oxide-bridge manganese cores such as the water-oxidizing complex of photosystem II[1] and catalase enzymes.[2] Second, Mn clusters often exhibit large, and sometimes abnormally large, spin values in the ground state and, combined with a large anisotropy, have led some of these species to be single-molecule magnets (SMMs). SMMs function as single-domain magnetic particles that, below their blocking temperature (T_B), exhibit the classical property of a magnet, namely, magnetization hysteresis. In addition, SMMs straddle the classical/quantum interface in also displaying quantum tunneling of magnetization (QTM)[3] and quantum phase interference.[4] Because a SMM derives its unusual properties from a combination of large ground-state spin (*S*) and large, easy-axis-type anisotropy due to a negative axial zero-field splitting (ZFS), *D*,[5] a primary goal in this area is to maximize *S* and |*D*|. Large *S* values arise from ferromagnetic or competing antiferromagnetic exchange. The first reported SMM was $[Mn_{12}O_{12}(O_2CMe)_{16}(H_2O)_4]$,[5] with $S = 10$ and $D = -0.50$ cm^{-1} $= -0.72$ K. Since then, a number of SMMs,

* Corresponding author. Tel.: +886 6 275 7575 × 65349.Fax: +886 6 274 0552. E-mail: hltsai@mail.ncku.edu.tw.
[†] National Cheng Kung University.
[‡] Laboratoire Louis Néel, CNRS.
[§] National Taiwan University.
[||] National Taiwan Normal University.

(1) Yachandra, V. L.; Sauer, K. P.; Klein, M. *Chem. Rev.* **1996**, *96*, 2927.
(2) Pecoraro, V. L. *Manganese Redox Enzymes*; VCH: New York, 1992.
(3) Friedman, J. R.; Sarachik, M. P.; Tejada, J.; Ziolo, R. *Phys. Rev. Lett.* **1996**, *76*, 3830.
(4) Wernsdorfer, W.; Sessoli, R. *Science* **1999**, *284*, 133.

10.1021/ic7013368 CCC: $40.75
Published on Web 02/22/2008

containing Mn;[6,7] V;[8] Fe;[9] Co;[10] Ni;[11] mixed-metal systems 3d−3d,[12] 3d−4d,[13] 3d−5d,[14] and 3d−4f;[15] and other oxidation levels of the Mn_{12} family,[16] have been reported with S values ranging from 3 to $^{83}/_{2}$.

Recently, the first exchange-coupled dimer of SMMs has demonstrated the feasibility of fine-tuning the quantum properties of these nanoscale magnetic materials.[17] An important future development for the SMM field is the discovery of synthetic schemes that can yield new molecules and families of related molecules with large spins or significant magnetoanisotropies. A large number of SMMs contain Mn^{III}, due to the combination of a large number of unpaired electrons on each high-spin, near-octahedral Mn^{III} ion and the Jahn–Teller (JT) distortion in the form of an axial elongation.[18] It is known that the Mn^{III} ion JT elongation plays an importance role in presence of SMM properties, and the orientations of JT elongation significantly affect the energy barrier in some Mn_{12} systems.[19] Thus, many current routes to SMMs culminate in Mn^{III}-containing complexes and exploit the associated large single-ion anisotropy.[20] One of the synthetic methodologies that has proved to be extremely successful in the synthesis of new polynuclear complexes is the reaction of a chelating ligand with a preformed Mn−carboxylate cluster that does not incorporate any chelate ligands. Some of the most successful starting materials employed for this purpose are the trinuclear μ_3-oxo complexes $[Mn_3O(O_2CR)_6(py)_3]^{n+}$ ($n = 0, 1$), which have afforded a variety of new complexes ranging in nuclearity from 3 to 22.[21]

The pyridine containing β-diketones, 1-phenyl-3-(2-pyridyl)propane-1,3-dione and 1-(2-pyridly)-3-(p-tolyl)propane-1,3-dione, are attractive for the above applications. The ligands have been know in organic chemistry for a long time,[22] but their uses to date in coordination chemistry have been very few.[23] Our own work with these ligands has now led to the preparation of four new compounds: [Mn_4O-

(5) (a) Sessoli, R.; Tsai, H. L.; Schake, A. R.; Wang, S.; Vincent, J. B.; Folting, K.; Gatteschi, D.; Christou, G.; Hendrickson, D. N. *J. Am. Chem. Soc.* **1993**, *115*, 1804. (b) Gatteschi, D.; Caneschi, A.; Pardi, L.; Sessoli, R. *Science* **1994**, *265*, 1054. (c) Christou, G.; Gatteschi, D.; Hendrickson, D. N.; Sessoli, R. *MRS Bull.* **2000**, *25*, 66 and references therein. (d) Tasiopoulos, A. J.; Vinslava, A.; Wernsdorfer, W.; Abboud, K. A.; Christou, G. *Angew. Chem., Int. Ed.* **2004**, *43*, 2117. (e) Coulon, C.; Miyasaka, H.; Clérac, R. *Struct. Bonding (Berlin)* **2006**, *122*, 163 and references therein.

(6) (a) Aubin, S. M. J.; Spagna, S.; Eppley, H. J.; Sager, R. E.; Christou, G.; Hendrickson, D. N. *Chem. Commun.* **1998**, 803. (b) Tsai, H. L.; Chen, D. M.; Yang, C. I.; Jwo, T. Y.; Wur, C. S.; Lee, G. H.; Wang, Y. *Inorg. Chem. Commun.* **2001**, *4*, 511. (c) Jones, L. F.; Rajaraman, G.; Brockman, J.; Murugesu, M.; Raftery, J.; Teat, S. J.; Wernsdorfer, W.; Christou, G.; Brechin, E. K.; Collison, D. *Chem.—Eur. J.* **2004**, *10*, 5180. (d) Murugesu, M.; Habrych, M.; Wernsdorfer, W.; Abboud, K. A.; Christou, G. *J. Am. Chem. Soc.* **2004**, *126*, 4766. (e) Ako, A. K.; Hewitt, I. J.; Mereacre, V.; Clérac, R.; Wernsdorfer, W.; Anson, C. E.; Powell, A. K. *Angew. Chem., Int. Ed.* **2006**, *45*, 4926.

(7) (a) Yang, C. I.; Lee, G. H.; Wur, C. S.; Lin, J. G.; Tsai, H. L. *Polyhedron.* **2005**, *24*, 2215. (b) Brechin, E. K.; Sanudo, E. C.; Wernsdorfer, W.; Boskovic, C.; Yoo, J.; Hendrickson, D. N.; Yamaguchi, A.; Ishimoto, H.; Concolino, T. E.; Rheingold, A. L.; Christou, G. *Inorg. Chem.* **2005**, *44*, 502. (c) Piligkos, S.; Rajaraman, G.; Soler, M.; Kirchner, N.; Slageren, J.; Bircher, R.; Parsons, S.; Guedel, H. U.; Kortus, J.; Wernsdorfer, W.; Christou, G.; Brechin, E. K. *J. Am. Chem. Soc.* **2005**, *127*, 5572. (d) Stamatatos, T. C.; Abboud, K. A.; Wernsdorfer, W.; Christou, G. *Angew. Chem., Int. Ed.* **2007**, *46*, 884. (e) Yang, C.-I.; Wernsdorfer, W.; Lee, G.-H.; Tsai, H.-L. *J. Am. Chem. Soc.* **2007**, *129*, 456.

(8) Castro, S. L.; Sun, Z.; Grant, C. M.; Bollinger, J. C.; Hendrickson, D. N.; Christou, G. *J. Am. Chem. Soc.* **1998**, *120*, 2365.

(9) (a) Barra, A. L.; Caneschi, A.; Cornia, A.; Fabrizi de Biani, F.; Gatteschi, D.; Sangregorio, C.; Sessoli, R. *J. Am. Chem. Soc.* **1999**, *121*, 5302. (b) Gatteschi, D.; Sessoli, R.; Cornia, A. *Chem. Commun.* **2000**, 725. (c) Oshio, H.; Hoshino, N.; Ito, T. *J. Am. Chem. Soc.* **2000**, *122*, 12602. (d) Powell, G. W.; Lancashire, H. N.; Brechin, E. K.; Collison, D.; Heath, S. L.; Mallah, T.; Wernsdorfer, W. *Angew. Chem., Int. Ed.* **2004**, *43*, 5772. (e) Accorsi, S.; Barra, A.-L.; Caneschi, A.; Chastanet, G.; Cornia, A.; Fabretti, A. C.; Gatteschi, D.; Mortalò, C.; Olivieri, E.; Parenti, P.; Rosa, P.; Sessoli, R.; Sorace, L.; Wernsdorfer, W.; Zobbi, L. *J. Am. Chem. Soc.* **2006**, *128*, 4742.

(10) (a) Young, E. C.; Hendrickson, D. N.; Wernsdorfer, W.; Nakano, M.; Zakharova, L. N.; Sommer, R. D.; Rheingold, A. R.; Ledezma-Gairaud, M.; Christou, G. *J. Appl. Phys.* **2002**, *91*, 7382. (b) Murrie, M.; Teat, S. J.; Stoeckli-Evans, H.; Güdel, H. U. *Angew. Chem., Int. Ed.* **2003**, *42*, 4653.

(11) (a) Ochsenbein, S. T.; Murrie, M.; Rusanov, E.; Stoeckli-Evans, H.; Sekime, C.; Güdel, H. U. *Inorg. Chem.* **2002**, *41*, 5133. (b) Moragues-Cánovas, M.; Helliwell, M.; Ricard, L.; Rivière, E.; Wernsdorfer, W.; Brechin, E. K.; Mallah, T. *Eur. J. Inorg. Chem.* **2004**, 2219. (c) Aromí, G.; Parsons, S.; Wernsdorfer, W.; Brechin, E. K.; McInnes, E. J. L. *Chem. Commun.* **2005**, 5038.

(12) (a) Oshio, H.; Nihei, M.; Yoshida, A.; Nojiri, H.; Nakano, M.; Yamaguchi, A.; Karaki, Y.; Ishimoto, H. *Chem.—Eur. J.* **2005**, *11*, 843. (b) Oshio, H.; Nihei, M.; Koizumi, S.; Shiga, T.; Nojiri, H.; Nakano, M.; Shirakawa, N.; Akatsu, M. *J. Am. Chem. Soc.* **2005**, *127*, 4568. (c) Yang, C. I.; Tsai, H. L.; Lee, G. H.; Wur, C. S.; Yang, S. F. *Chem. Lett.* **2005**, 288.

(13) Sokol, J. J.; Hee, A. G.; Long, J. R. *J. Am. Chem. Soc.* **2002**, *124*, 7656.

(14) Schelter, E. J.; Prosvirin, A. V.; Dunbar, K. R. *J. Am. Chem. Soc.* **2004**, *126*, 15004.

(15) (a) Osa, S.; Kido, T.; Matsumoto, N.; Pochaba, N. A.; Mrozinski, J. *J. Am. Chem. Soc.* **2004**, *126*, 420. (b) Zaleski, C. M.; Depperman, E. C.; Kampf, J. W.; Kirk, M. L.; Pecoraro, V. L. *Angew. Chem., Int. Ed.* **2004**, *43*, 3912. (c) Mishra, A.; Wernsdorfer, W.; Abboud, K. A.; Christou, G. *J. Am. Chem. Soc.* **2004**, *126*, 15648. (d) Mishra, A.; Wernsdorfer, W.; Parsons, S.; Christou, G.; Brechin, E. K. *Chem. Commun.* **2005**, 2086.

(16) (a) Eppley, H. J.; Tsai, H. L.; de Vries, N.; Folting, K.; Christou, G.; Hendrickson, D. N. *J. Am. Chem. Soc.* **1995**, *117*, 301. (b) Chakov, N. E.; Soler, M.; Wernsdorfer, W.; Abboud, K. A.; Christou, G. *Inorg. Chem.* **2005**, *44*, 5304. (c) Tsai, H. L.; Jwo, T. Y.; Lee, G. H.; Wang, Y. *Chem. Lett.* **2000**, 346. (d) Tsai, H. L.; Shiao, H. A.; Jwo, T. Y.; Yang, C. I.; Wur, C. S.; Lee, G. H. *Polyhedron* **2005**, *24*, 2205.

(17) (a) Wernsdorfer, W.; Aliaga-Alcalde, N.; Hendrickson, D. N.; Christou, G. *Nature* **2002**, *416*, 406. (b) Hill, S.; Edwards, R.; Aliaga-Alcalde, N.; Christou, G. *Science* **2003**, *302*, 1015.

(18) Cotton, F. A.; Wilkinson, G. *Advanced Inorganic Chemistry*, 4th ed.; John Wiley and Sons: New York, 1980.

(19) Soler, M.; Wernsdorfer, W.; Sun, Z.; Huffman, J. C.; Hendrickson, D. N.; Christou, G. *Chem. Commun.* **2003**, 2672.

(20) (a) Boskovic, C.; Wernsdorfer, W.; Folting, K.; Huffman, J. C.; Hendrickson, D. N.; Christou, G. *Inorg. Chem.* **2002**, *41*, 5107. (b) Brechin, E. K.; Soler, M.; Davidson, J.; Hendrickson, D. N.; Parsons, S.; Christou, G. *Chem. Commun.* **2002**, 2252.

(21) (a) Aromi, G.; Aubin, S. M.; Bolcar, M. A.; Christou, G.; Eppley, H. J.; Folting, K.; Hendrickson, D. N.; Huffman, J. C.; Squire, R. C.; Tsai, H.-L.; Wang, S.; Wemple, M. W. *Polyhedron* **1998**, *17*, 3005. (b) Boskovic, C.; Wernsdorfer, W.; Folting, K.; Huffman, J. C.; Hendrickson, D. N.; Christou, G. *Inorg. Chem.* **2002**, *41*, 5107. (c) Murugesu, M.; Raftery, J.; Wernsdorfer, W.; Christou, G.; Brechin, E. K. *Inorg. Chem.* **2004**, *43*, 4203. (d) Sañudo, E. C.; Wernsdorfer, W.; W; Abboud, W.; Christou, G. *Inorg. Chem.* **2004**, *43*, 4137. (e) Stamatatos, T. C.; Foguet-Albiol, D.; Stoumpos, C. C.; Raptopoulou, C. P.; Terzis, A.; Wernsdorfer, W.; Perlepes, S. P.; Christou, G. *J. Am. Chem. Soc.* **2005**, *127*, 15380.

(22) Levine, R. L.; Sneed, J. K. *J. Am. Chem. Soc.* **1951**, *73*, 5614.

(23) (a) Saalfrank, R. W.; Dresel, A.; Seitz, V.; Trummer, S.; Hampel, F.; Teichert, M.; Stalke, D.; Stalk, C.; Daub, J.; Schunemann, V.; Trautwein, A. X. *Chem.—Eur. J.* **1997**, *3*, 2058. (b) Saalfrank, R. W.; Seitz, V.; Caulder, D. L.; Raymond, K. N.; Teichert, M.; Sheldrick, G. M. *Eur. J. Inorg. Chem.* **1998**, 1313. (c) Saalfrank, R. W.; Low, N.; Trummer, S.; Sheldrick, G. M.; Teichert, M.; Stalke, D. *Eur. J. Inorg. Chem.* **1998**, 599. (d) Bruck, S.; Hider, M.; Junk, P. C.; Kynast, U. H. *Inorg. Chem. Commun.* **2000**, *3*, 666. (e) Saalfrank, R. W.; Seitz, V.; t-lrmer, F.; Heinemann, W.; Gobel, G.; Herbst-lrmer, R. *J. Chem. Soc., Dalton Trans.* **2001**, 599.

$(O_2CCCl_3)_6(L^1)_2]$ (**1**), $[Mn_4O(O_2CCCl_3)_6L_2^2]$ (**2**), $[Mn_6O_2$-$(O_2CPh)_8(L^1)_3]$ (**3**), and $[Mn_6O_2(O_2CPh)_8L_3^2]$ (**4**), **3** and **4** having an unprecedented hexanuclear Mn_6 topology and structure. The synthesis, structure, and magnetic properties of these complexes are reported as follows.

Experimental Section

Synthesis. All solvents and reagents were used as received; no purification was necessary. All reactions were performed under aerobic conditions. $[Mn_3O(O_2CCCl_3)(H_2O)_3]$[24] and $[Mn_3O(O_2CPh)(py)_2(H_2O)]$[25] were prepared as described in the literature, and the ligands of HL^1 and HL^2 were prepared via a Claisen condensation reaction as previously reported.[22]

1-phenyl-3-(2-pyridyl)propane-1,3-dione (HL^1). Yield: 63% yellow needles from dichloromethane. mp: 84∼85 °C. ^{1}H NMR (500 MHz, d_6-acetone, 25 °C): δ 7.58 (t, 2H, J = 7.3 Hz), 7.60 (dd, 1H, J = 7.8, 5.3 Hz), 7.64 (t, 1H, J = 7.3 Hz), 7.66 (s, 1H), 8.02 (t, 1H, J = 7.8 Hz), 8.09 (d, 2H, J = 7.3 Hz), 8.17 (d, 1H, J = 7.8 Hz), 8.76 (d, 1H, J = 5.3 Hz), 16.67 (s, 1H). ^{13}C NMR (125 MHz, d_6-acetone, 25 °C): δ 93.9, 122.7, 127.7, 128.1, 129.8, 133.8, 136.0, 138.2, 150.4, 153.0, 185.4, 186.6. IR: 1600 cm^{-1} (C═O). Anal. calcd (found) for $C_{14}H_{11}NO_2$: C, 74.65 (74.54); H, 4.92 (5.01); N, 6.22 (6.28). MS (70 eV, EI; %): m/z 225 (38) [M^+].

1-(2-pyridly)-3-(*p*-tolyl)propane-1,3-dione (HL^2). Yield: 72% yellow needles from dichloromethane. mp: 62∼63 °C. ^{1}H NMR (400 MHz, d_6-acetone, 25 °C): δ 2.39 (s, 3H), 7.40 (d, 2H, J = 8.1 Hz), 7.64 (s, 1H), 7.7 (ddd, 1H, J = 7.7, 4.7, 1.3 Hz), 8.02 (d, 2H, J = 8.1 Hz), 8.07 (td, 1H, J = 7.6, 1.5 Hz), 8.17 (d 1H, J = 7.7 Hz), 8.77 (d, 1H, J = 4.7 Hz), 17.16 (s, 1H). ^{13}C NMR (125 MHz, d_6-acetone, 25 °C): δ 21.5, 93.5, 122.6, 127.6, 128.2, 130.4, 133.3, 138.2, 144.7, 150.4, 153.0, 184.6, 187.0. IR: 1600 cm^{-1} (C═O). Anal. calcd (found) for $C_{15}H_{13}NO_2$: C, 75.29 (75.24); H, 5.48 (5.45); N, 5.85 (5.78). MS (70 eV, EI; %): m/z 239 (46) [M^+].

$[Mn_4O(O_2CCCl_3)_6(L^1)_2]$ (1). $[Mn_3O(O_2CCCl_3)_6(H_2O)_3]$ (0.125 g 0.101 mmol) was dissolved in 2.0 mL of Et_2O, followed by the addition of 50.0 mL of CH_2Cl_2, and the solid HL^1 (0.034 g, 0.151 mmol) was added. A yellow-brown solution was obtained after stirring for 10 min. The solution was filtered to eliminate any remaining solid, and the filtrate was layered with two volumes of hexane to slowly give well-formed brown crystals. After one week, the crystals that had formed were isolated by filtration, washed with hexane, and dried in vacuo. Yield: 65% (based on Mn). The sample for crystallography was maintained in contact with the mother liquor to avoid solvent loss, and it was identified as **1**·$2CH_2Cl_2$. Anal. calcd (found) for $[Mn_4O(O_2CCCl_3)_6(L^1)_2]$ (**1**): C, 28.97 (28.43); H, 1.22 (1.27); N, 1.68 (1.60). IR data (KBr disk, cm^{-1}): 1692 (vs), 1622 (s), 1587 (s), 1557 (s), 1532 (s), 1509 (s), 1487 (s), 1467 (s), 1449 (m), 1436 (m), 1458 (m), 1317 (m), 1284 (vs), 1131 (w), 1044 (w), 1018 (w), 945 (w), 837 (vs), 769 (m), 742 (s), 712 (s), 683 (vs), 629 (m), 590 (m).

$[Mn_4O(O_2CCCl_3)_6(L^2)_2]$ (2). The procedure was the same as that employed for complex **1**, except that HL^2 (0.036 g, 0.151 mmol) was added. Brown crystals were again obtained. Yield: 50% (based on Mn). The sample for crystallography was maintained in contact with the mother liquor to avoid solvent loss, and it was identified as **2**·$2CH_2Cl_2$·H_2O. Anal. calcd (found) for $[Mn_4O(O_2CCCl_3)_6(L^2)_2]$ (**2**): C, 29.91 (29.94); H, 1.43 (1.51); N, 1.66 (1.71). IR data (KBr disk, cm^{-1}): 2919 (w), 1669 (vs), 1604 (s), 1578 (s), 1551 (vs), 1519 (vs), 1489 (vs), 1467 (s), 1439 (s), 1357 (s), 1319 (s), 1302 (s), 1262 (m), 1240 (w), 1189 (m), 1644 (w), 1124 (w), 1076 (w), 1049 (m), 943 (m), 837 (s), 780 (s), 737 (s), 682 (s), 637 (m), 589 (w).

$[Mn_6O_2(O_2CPh)_8(L^1)_3]$ (3). $[Mn_3O(O_2CPh)_6(py)_2(H_2O)]$ (0.498 g, 0.460 mmol) was dissolved in 30.0 mL of CH_2Cl_2, and the solid HL^1 (0.169 g, 0.751 mmol) was added. A yellow-brown solution was obtained after stirring for 10 min. The solution was filtered to eliminate any remaining solid, and the filtrate was layered with two volumes of a 1:1 hexane/Et_2O solution to slowly give well-formed brown crystals. The sample for crystallography was maintained in contact with the mother liquor to avoid solvent loss, and it was identified as **3**·$1.5CH_2Cl_2$·Et_2O·H_2O. The yield was 53% (based on Mn). Anal. calcd (found) for $[Mn_6O_2(O_2CPh)_8(L^1)_3]$·$H_2O$ (**3**·H_2O): C, 58.23 (57.21); H, 3.59 (3.77); N, 2.08 (2.04). IR data (KBr disk, cm^{-1}): 3062 (w), 1605 (s), 1561 (s), 1509 (s), 1467 (s), 1405 (w), 1382 (w), 1285 (s), 1204 (vs), 1148 (s), 1044 (w), 1019 (w), 942 (w), 845 (m), 799 (m), 726 (s), 657 (m), 636 (m), 589 (w), 558 (w), 522 (w).

$[Mn_6O_2(O_2CPh)_8(L^2)_3]$ (4). This complex was prepared in the same manner as complex **3**, except that HL^2 (0.169 g, 0.751 mmol) was used in place of HL^1. Brown crystals were obtained. Yield: 40% (based on Mn). The sample for crystallography was maintained in contact with the mother liquor to avoid solvent loss, and it was identified as **4**·$2CH_2Cl_2$. Anal. calcd (found) for $[Mn_6O_2(O_2CPh)_8(L^2)_3]$ (**4**): C, 59.31 (59.24); H, 3.75 (3.99); N, 2.05 (2.05). IR data (KBr disk, cm^{-1}): 3062 (w), 2922 (w), 1604 (s), 1561 (s), 1499 (s), 1445 (s), 1398 (vs), 1291 (m), 1174 (w), 1068 (w), 1044 (w), 1025 (w), 942 (w), 839 (w), 770 (w), 716 (s), 676 (m), 632 (m), 589 (w), 513 (w).

X-Ray Crystallography. Data collection parameters are listed in Table 1. Diffraction measurements for complexes **1**·$2CH_2Cl_2$, **2**·$2CH_2Cl_2$·H_2O, **3**·$1.5CH_2Cl_2$·Et_2O·H_2O, and **4**·$2CH_2Cl_2$ were carried out using a Brucker-Nonius Kappa CCD diffractometer with graphite-monochromated Mo Kα radiation (λ = 0.7107 Å). Cell parameters were retrieved and refined using the DENZO-SMN[26] software on all reflections. Data reduction was performed with the DENZO-SMN software. Structure analysis was made using the SHELXTL program on a personal computer. For complex **1**·$2CH_2Cl_2$, the SHELXS-97 program was used for structural solution, and the results were refined by full-matrix least-squares on F^2 values, while the structures of **2**·$2CH_2Cl_2$·H_2O, **3**·$1.5CH_2Cl_2$·Et_2O·H_2O, and **4**·$2CH_2Cl_2$ were solved using the SHELXS-86[27] program and refined using the SHELXL-97[28] program by full-matrix least-squares on F^2 values. All nonhydrogen atoms were refined anisotropically, whereas the hydrogen atoms were placed in ideal, calculated positions, with isotropic thermal parameters riding on their respective carbon atoms. For complex **1**·$2CH_2Cl_2$, the asymmetric unit consists of a Mn_4 molecule and two CH_2Cl_2 solvent molecules. One of six $CCCl_3$ groups of $Cl_3CCO_2^-$ligands showed rotational disordering of its Cl atoms, and the occupancies of Cl(17), Cl(17A), Cl(18), and Cl(18A) were refined to 75:25 and 75:25, respectively. For **2**·$2CH_2Cl_2$·H_2O, the asymmetric unit consists of a Mn_4 molecule, two CH_2Cl_2 molecules, and one molecule of water. The $Cl_3CCO_2^-$ ligands showed highly rotational

(24) Tsai, H.-L.; Jwo, T. Y.; Yang, C. I.; Wur, C. S.; Lee, G. H.; Wang, Y. *J. Chin. Chem. Soc.* **2003**, *50*, 1139.
(25) Vincent, J. B.; Chang, H. R.; Folting, K.; Huffman, J. C.; Christou, G.; Hendrickson, D. N. *J. Am. Chem. Soc.* **1987**, *109*, 5703.
(26) DENZO-SMN: Otwinowsky, Z.; Minor, W. Processing of X-ray Diffraction Data Collected in Oscillation Mode. In *Methods in Enzymology*; Carter, C. W., Jr., Sweet, R. M., Eds.; Academic Press: New York, 1997; Vol. 276: Macromolecular Crystllography, Part A, pp 307–326.
(27) Sheldrick, G. M. *SHELXL-97*; University of Gottingen: Gottingen, Germany, 1997.
(28) Sheldrick, G. M. *SHELXL-86*; University of Gottingen: Gottingen, Germany, 1986.

Table 1. Crystallographic Data for **1**, **2**, **3**, and **4**

	1·2CH_2Cl_2	**2**·2CH_2Cl_2·H_2O	**3**·1.5CH_2Cl_2·Et_2O·H_2O	**4**·2CH_2Cl_2
formula	$C_{42}H_{24}Cl_{22}Mn_4N_2O_{17}$	$C_{44}H_{30}Cl_{22}Mn_4N_2O_{18}$	$C_{103.5}H_{85}Cl_3Mn_6N_3O_{26}$	$C_{103}H_{80}Cl_4Mn_6N_3O_{24}$
fw	1828.29	1874.36	2222.74	2215.14
cryst syst	triclinic	monoclinic	monoclinic	monoclinic
space group	$P\bar{1}$	$P2_1/c$	$P2_1/n$	$P2_1/n$
a/Å	13.4906 (2)	14.2480(2)	16.20160 (10)	15.9030(2)
b/Å	13.7032 (3)	23.4740(3)	34.6578 (3)	41.1760(5)
c/Å	19.1591 (4)	21.1190(4)	17.6014 (2)	17.3400(3)
α/deg	73.4925 (11)	90	90	90
β/deg	78.6950 (10)	90.8210(10)	98.11	97.8750(10)
γ/deg	80.5114 (6)	90	90	90
V/Å^3	3307.45 (11)	7062.68(19)	9784.53(15)	11247.5(3)
Z	2	4	4	4
T/K	150 (1)	200 (2)	200 (2)	200 (2)
wavelength (Å)	0.7103	0.7103	0.7103	0.7103
ρ_{calcd}/g cm^{-3}	1.836	1.763	1.509	1.308
μ/mm^{-1}	1.698	1.594	0.912	0.815
$(\Delta\rho)_{max}$, $(\Delta\rho)_{min}$/*e* Å^{-3}	2.274,−1.074	0.841,−0.833	1.012,−1.020	1.460,−0.760
R_1,[a] wR_2[b] (all data)	0.1230, 0.2722	0.1492, 0.2878	0.1285, 0.2401	0.1304, 0.2620
R_1,[a] wR_2[b] ($I > 2\sigma$ (I))	0.0888, 0.2341	0.0965, 0.2472	0.0755, 0.1979	0.0827, 0.2321

[a] $R_1 = \sum||F_o| - |F_c||/\sum|F_o|$. [b] $wR_2 = [\sum[w(F_o^2 - F_c^2)^2]/\sum[w(F_o^2)^2]]^{1/2}$.

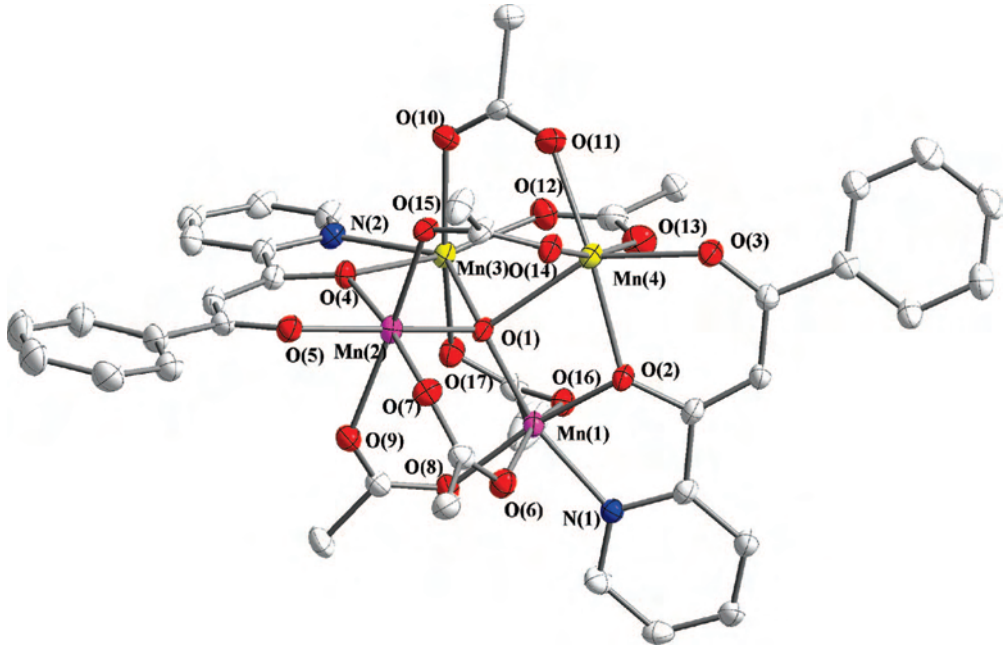

Figure 1. ORTEP drawings of **1** with thermal ellipsoids set at 30% probability. The Cl atoms, H atoms, and solvated molecules have been omitted for clarity.

disordering of their Cl atoms. Data for **3**·1.5CH_2Cl_2·Et_2O·H_2O is as follows: the asymmetric unit consists of a Mn_6 molecule, 1.5 CH_2Cl_2 molecules, one Et_2O molecule, and one water solvent molecule. For **4**·2CH_2Cl_2, the asymmetric unit consists of a Mn_6 molecule and two CH_2Cl_2 molecules, and the phenyl rings of one diketonate and one benzoate are disordered as well as one pyridine ring of diketonate.

Physical Measurements. Infrared spectra were recorded in the solid state (KBr pellets) on a Nicolet Magna 550 FTIR spectrometer in the 400–4000 cm^{-1} range. Elemental analyses have been carried out using an Elementar vario EL III analyzer. Variable-temperature DC magnetic susceptibility measurements and AC magnetic susceptibility were collected on microcrystalline samples, restrained in eicosane to prevent torquing, on a Quantum Design MPMS-XL SQUID magnetometer equipped with a 7.0 T magnet and operating in the range of 1.8–300.0 K. Diamagnetic corrections were estimated from Pascal's constants[29] and subtracted from the experimental susceptibility data to obtain the molar paramagnetic susceptibility of the compounds.

Other Studies. ^{1}H NMR and ^{13}C NMR spectra were measured in a d_6-acetone solution on Bruker AMX-400 (400 MHz) or Avance-500 (500 MHz) NMR spectrometers with tetramethylsilane as the internal standard. The electron impact (EI)-mass spectra were recorded on a Bruker APEX II. Melting points of HL^1 and HL^2 were measured using a capillary melting point apparatus.

Results and Discussion

Synthesis. The reaction of a $[Mn_3O(O_2CR)_6S_3]^{0,+}$ (S = py, H_2O, etc.) complex with a chelating ligand represents a commonly employed and successful route to a wide range of higher nuclearity clusters of Mn. For example, the use of

(29) Boudreaux, E. A.; Mulay, L. N. *Theory and Application of Molecular Paramagnetism*; J. Wiley & Sons: New York, 1976; p 491.

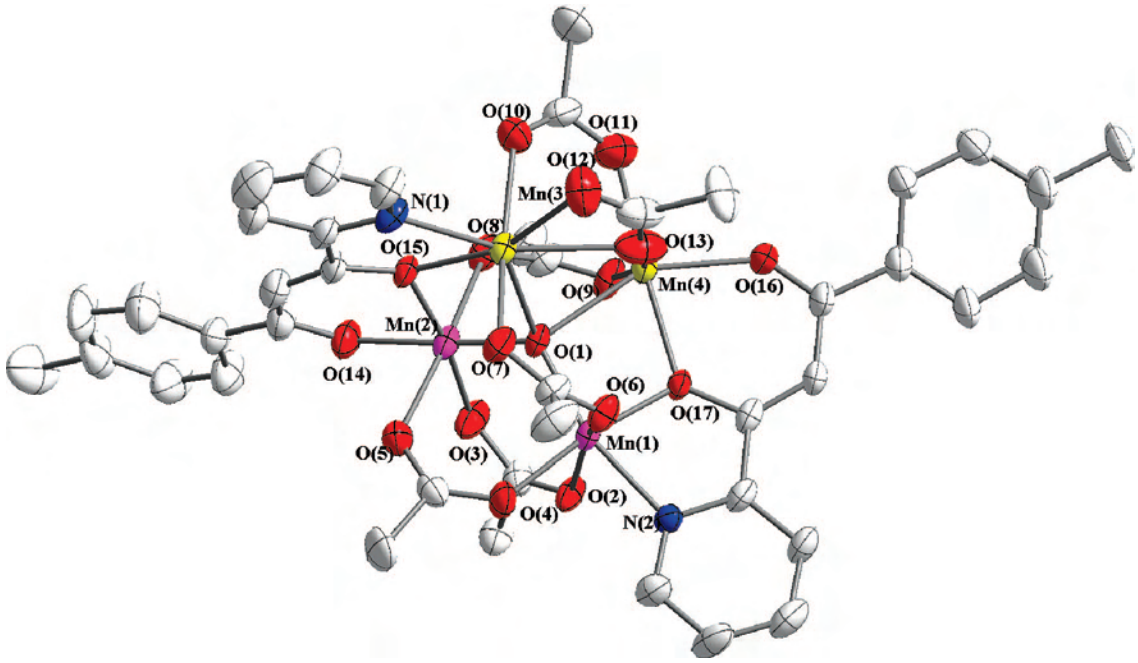

Figure 2. ORTEP drawings of **2** with thermal ellipsoids set at 30% probability. The Cl atoms, H atoms, and solvated molecules have been omitted for clarity.

dibenzolymethane (dbmH) or 2-hydroxymethylpyridine has led to a large variety of products, depending on the precise reaction conditions and ratios of the reactants, including Mn_4,[30] Mn_6,[31] Mn_7,[32,33] Mn_{10},[33] and Mn_{12}[34] clusters. $[Mn_3O(O_2CR)_6S_3]$ has been employed in reactions with pyridyl-substituted β-diketone in CH_2Cl_2.

The synthesis of ligands HL^1 and HL^2 has been reported previously.[22] The pyridine-containing β-diketone ligands have been prepared using the Claisen condensation reaction. The reaction of ethyl picolinate with sodium ethoxide and acetophenone in a 1:1:1 molar ratio in anhydrous ether affords, along with acetic acid, 1-phenyl-3-pyridin-2-yl-propane-1,3-dione (HL^1). A similar reaction was carried out starting with *p*-methylacetophenone instead of acetophenone to yield 1-(2-pyridly)-3-(*p*-tolyl)propane-1,3-dione (HL^2). The identity of HL^1 and HL^2 were confirmed by IR, MS, and ^1H NMR spectroscopy. The NMR assignments were made on the basis of two-dimensional $^1H-^1H$ correlation spectroscopy.

Treatments of $[Mn_3O(O_2CCCl_3)(H_2O)_3]$ with ~1.5 equiv of HL^1 and HL^2 in a CH_2Cl_2/Et_2O mixture gave a color change to yellow-brown, and followed by filtration, layered the resulting solution with hexane and afforded crystalline $[Mn_4O(O_2CCCl_3)_6(L^1)_2]$ (**1**) and $[Mn_4O(O_2CCCl_3)_6(L^2)_2]$ (**2**) in 65% and 50% yields, respectively, after one week. The reactions are summarized in eq 1.

$$2[Mn_3O(O_2CCCl_3)_6(H_2O)_3 + 2HL \rightarrow [Mn_4O(O_2CCCl_3)_6(L)_2] + 2Mn^3 + 7H_2O + 6CCl_3CO_2^- \ (L = L^1 \text{ or } L^2) \quad (1)$$

Those reactions involve a reduction state of the Mn center from an average oxidation state of +2.67 in the $Mn^{II}Mn^{III}_2$ starting complex to +2.5 in the $Mn^{II}_2Mn^{III}_2$ product, accompanied by fragmentation and structural rearrangement to yield the new complexes. Bond valence sum calculations on **1** and **2** gave excellent agreement with the Mn^{II} and Mn^{III} oxidation states assigned from structures and formulas.

Complexes **3** and **4** were prepared from a similar reaction employing the benzoate $Mn^{II}Mn^{III}_2$ complex of $[Mn_3O(O_2CPh)(py)_2(H_2O)]$. Reaction of this complex with ~1.5 equiv of HL in CH_2Cl_2, followed by filtration, layered the resulting solution with hexane and afforded crystalline $[Mn_6O_2(O_2CPh)_8(L^1)_3]$ and $[Mn_6O_2(O_2CPh)_8(L^2)_3]$ in 53% and 50% yields, respectively, after one week. The use of more than 2 or less than 1.5 equiv of HL reduced the yield of the final product. The formations of complexes were summarized in eq 2.

$$3[Mn_3O(O_2CPh)_6(py)_2(H_2O)] + 3HL \rightarrow [Mn_6O_2(O_2CPh)_8(L)_3] + 3Mn^{3+} + 4H_2O + 10PhCO_2^- + 6py + H^+ \ (L = L^1 \text{ or } L^2) \quad (2)$$

Charge considerations and the inspection of metric parameters indicate that complexes **3** and **4** are mixed-valence $Mn^{II}_3Mn^{III}_3$ with a trapped-valence situation (*vide infra*). The reaction involves a reduction state of the Mn center from an average oxidation state of +2.67 in the $Mn^{II}Mn^{III}_2$ starting complex to +2.5 in the $Mn^{II}_3Mn^{III}_3$ product. Again, for **3** and **4**, clearly, the overall conversion of $[Mn_3O(O_2CPh)_6(py)_2(H_2O)]$ into these product must involve a complicated

(30) Aubin, S. M. J.; Wemple, M. W.; Adams, D. M.; Tsai, H. L.; Christou, G.; Hendrickson, D. N. *J. Am. Chem. Soc.* **1996**, *118*, 7746.
(31) Abbati, G. L.; Cornia, A.; Fabretti, A. C.; Caneschi, A.; Gatteschi, D. *Inorg. Chem.* **1998**, *37*, 1430.
(32) Abbati, G. L.; Cornia, A.; Fabretti, A. C.; Caneschi, A.; Gatteschi, D. *Inorg. Chem.* **1998**, *37*, 3759.
(33) Harden, N. C.; Bolcar, M. A.; Wernsdorfer, W.; Abboud, K. A.; Streib, W. E.; Christou, G. *Inorg. Chem.* **2003**, *42*, 7067.
(34) Boskovic, C.; Brechin, E.; Streib, W. E.; Folting, K.; Bollinger, J. C.; Hendrickson, D. N.; Christou, G. *J. Am. Chem. Soc.* **2002**, *124*, 3725.

Table 2. Selected bond distances (Å) and angles (deg) for complexes **1**·$2CH_2Cl_2$ and **2**·$2CH_2Cl_2$·H_2O

1·$2CH_2Cl_2$				**2**·$2CH_2Cl_2$·H_2O			
Mn(1)-O(1)	1.868(5)	Mn(1)-O(2)	1.923(5)	Mn(1)-O(1)	1.890(5)	Mn(2)-O(1)	1.853(5)
Mn(1)-O(8)	1.974(6)	Mn(1)-N(1)	2.021(6)	Mn(1)-O(17)	1.926(5)	Mn(2)-O(14)	1.932(6)
Mn(1)-O(16)	2.161(6)	Mn(1)-O(6)	2.257(6)	Mn(1)-O(4)	1.937(6)	Mn(2)-O(15)	1.940(5)
Mn(1)-Mn(4)	3.2141(17)	Mn(1)-Mn(2)	3.2345(16)	Mn(1)-N(2)	2.036(6)	Mn(2)-O(3)	1.963(6)
Mn(2)-O(1)	1.884(5)	Mn(2)-O(4)	1.915(5)	Mn(1)-O(6)	2.166(6)	Mn(2)-O(8)	2.150(6)
Mn(2)-O(5)	1.934(6)	Mn(2)-O(7)	1.964(6)	Mn(1)-O(2)	2.283(5)	Mn(2)-O(5)	2.214(7)
Mn(2)-O(15)	2.140(6)	Mn(2)-O(9)	2.195(6)	Mn(3)-O(7)	2.148(6)	Mn(4)-O(11)	2.079(7)
Mn(2)-Mn(3)	3.2291(17)	Mn(3)-O(12)	2.090(6)	Mn(3)-O(15)	2.168(5)	Mn(4)-O(16)	2.098(5)
Mn(3)-O(17)	2.147(6)	Mn(3)-O(4)	2.193(5)	Mn(3)-O(10)	2.258(7)	Mn(4)-O(17)	2.136(5)
Mn(3)-O(10)	2.211(6)	Mn(3)-N(2)	2.262(7)	Mn(3)-N(1)	2.273(7)	Mn(4)-O(9)	2.151(6)
Mn(3)-O(1)	2.304(5)	Mn(4)-O(11)	2.109(6)	Mn(3)-O(12)	2.291(8)	Mn(4)-O(13)	2.208(8)
Mn(4)-O(3)	2.159(6)	Mn(4)-O(13)	2.160(7)	Mn(3)-O(1)	2.391(5)	Mn(4)-O(1)	2.322(5)
Mn(4)-O(2)	2.163(5)	Mn(4)-O(14)	2.173(6)	Mn(3)-O(13)	2.401(10)		
Mn(4)-O(1)	2.346(5)						
				O(1)-Mn(1)-O(17)	85.3(2)	O(11)-Mn(4)-O(16)	98.9(3)
O(2)-Mn(1)-O(2)	86.2(2)	O(1)-Mn(1)-O(8)	101.3(2)	O(1)-Mn(1)-O(4)	101.9(2)	O(11)-Mn(4)-O(17)	171.6(3)
O(2)-Mn(1)-O(8)	171.0(2)	O(1)-Mn(1)-N(1)	165.8(2)	O(17)-Mn(1)-O(4)	171.9(2)	O(16)-Mn(4)-O(17)	79.2(2)
O(2)-Mn(1)-N(1)	80.0(2)	O(8)-Ma(1)-N(1)	92.8(3)	O(1)-Mn(1)-N(2)	164.1(2)	O(11)-Mn(4)-O(9)	87.1(3)
O(1)-Mn(1)-O(16)	97.1(2)	O(2)-Mn(1)-O(16)	98.7(2)	O(17)-Mn(1)-N(2)	79.0(2)	O(16)-Mn(4)-O(9)	99.1(3)
O(8)-Mn(1)-O(16)	85.5(2)	N(1)-Mn(1)-O(16)	81.8(2)	O(4)-Mn(1)-N(2)	93.9(2)	O(17)-Mn(4)-O(9)	101.3(2)
O(1)-Mn(1)-O(6)	97.4(2)	O(2)-Mn(1)-O(6)	90.2 (2)	O(1)-Mn(1)-O(6)	97.7(2)	O(11)-Mn(4)-O(13)	84.1(3)
O(8)-Mn(1)-O(6)	83.9(2)	N(1)-Mn(1)-O(6)	86.1(2)	O(17)-Mn(1)-O(6)	98.3(2)	O(16)-Mn(4)-O(13)	98.2(3)
O(16)-Mn(1)-O(6)	163.4(2)	O(1)-Mn(1)-Mn(4)	46.17(16)	O(4)-Mn(1)-O(6)	84.6(3)	O(17)-Mn(4)-O(13)	88.1(2)
O(2)-Mn(1)-Mn(4)	40.85(16)	O(8)-Mn(1)-Mn(4)	147.27 (17)	N(2)-Mn(1)-O(6)	82.5(2)	O(9)-Mn(4)-O(13)	161.6(3)
N(1)-Mn(1)-Mn(4)	119.63 (19)	O(16)-Mn(1)-Mn(4)	94.14 (16)	O(1)-Mn(1)-O(2)	96.3(2)	O(11)-Mn(4)-O(1)	110.5(2)
O(6)-Mn(1)-Mn(4)	101.70 (17)	O(1)-Mn(1)-Mn(2)	30.60(17)	O(17)-Mn(1)-O(2)	90.5(2)	O(16)-Mn(4)-O(1)	149.8(2)
O(2)-Mn(1)-Mn(2)	102.41(16)	O(8)-Mn(1)-Mn(2)	82.23(17)	O(4)-Mn(1)-O(2)	85.0(2)	O(17)-Mn(4)-O(1)	70.73(17)
N(1)-Mn(1)-Mn(2)	157.56 (19)	O(16)-Mn(1)-Mn(2)	119.31(15)	N(2)-Mn(1)-O(2)	86.2(2)	O(9)-Mn(4)-O(1)	89.6(2)
O(6)-Mn(1)-Mn(2)	71.71(15)	Mn(4)-Mn(1)-Mn(2)	69.46(4)	O(6)-Mn(1)-O(2)	164.0(2)	O(13)-Mn(4)-O(1)	78.5(3)
O(1)-Mn(2)-O(4)	85.7 (2)	O(1)-Mn(2)-O(5)	172.3(2)	O(1)-Mn(1)-Mn(4)	45.47(15)	O(11)-Mn(4)-Mn(1)	144.6(2)
O(4)-Mn(2)-O(5)	87.5(2)	O(1)-Mn(2)-O(7)	99.0(2)	O(17)-Mn(1)-Mn(4)	39.97(14)	O(16)-Mn(4)-Mn(1)	114.30(17)
O(4)-Mn(2)-O(7)	174.0(2)	O(5)-Mn(2)-O(7)	87.5(2)	O(4)-Mn(1)-Mn(4)	147.40(18)	O(17)-Mn(4)-Mn(1)	35.39(13)
O(1)-Mn(2)-O(15)	93.3(2)	O(4)-Mn(2)-O(15)	97.2 (2)	N(2)-Mn(1)-Mn(4)	118.69(18)	O(9)-Mn(4)-Mn(1)	99.01(19)
O(5)-Mn(2)-O(15)	91.1(2)	o(7)-Mn (2)-O(15)	86.4 (2)	O(6)-Mn(1)-Mn(4)	97.85(18)	O(13)-Mn(4)-Mn(1)	79.4(2)
O(1)-Mn(2)-O(9)	93.0(2)	O(4)-Ma(2)-O(9)	87.9(2)	O(2)-Mn(1)-Mn(4)	97.47(16)	O(1)-Mn(4)-Mn(1)	35.47(11)
O(5)-Mn(2)-O(9)	83.2(2)	O(7)-Mn(2)-O(9)	88.2(2)	O(1)-Mn(2)-O(14)	173.8(3)	C(6)-Cl(8A)-Cl(9A)	50.5(11)
O(15)-Mn(2)-O(9)	172.2(2)	O(1)-Mn(2)-Mn(3)	44.57(16)	O(1)-Mn(2)-O(15)	86.6(2)	C(6)-Cl(9A)-Cl(8A)	51.8(12)
				O(14)-Mn(2)-O(15)	87.4(2)	Mn(2)-O(1)-Mn(1)	119.9(3)
				O(1)-Mn(2)-O(3)	99.8(2)	Mn(2)-O(1)-Mn(4)	123.1(3)
				O(14)-Mn(2)-O(3)	86.0(3)	Mn(1)-O(1)-Mn(4)	99.06(19)
				O(15)-Mn(2)-O(3)	172.3(2)	Mn(2)-O(1)-Mn(3)	99.28(18)
				O(1)-Mn(2)-O(8)	92.6(2)	Mn(1)-O(1)-Mn(3)	121.6(2)
				O(14)-Mn(2)-O(8)	89.5(3)	Mn(4)-O(1)-Mn(3)	92.19(18)
				O(15)-Mn(2)-O(8)	95.3(2)	O(14)-Mn(2)-O(5)	85.4(3)
				O(3)-Mn(2)-O(8)	88.7(3)	O(15)-Mn(2)-O(5)	87.6(3)
				O(1)-Mn(2)-O(5)	92.8(2)	O(3)-Mn(2)-O(5)	87.9(3)
				O(8)-Mn(2)-O(5)	174.0(3)	O(7)-Mn(3)-O(1)	86.6(2)
				O(7)-Mn(3)-O(15)	102.4(2)	O(15)-Mn(3)-O(1)	69.42(17)
				O(7)-Mn(3)-O(10)	169.8(3)	O(10)-Mn(3)-O(1)	101.7(2)
				O(15)-Mn(3)-O(10)	86.1(2)	N(1)-Mn(3)-O(1)	134.9(2)
				O(7)-Mn(3)-N(1)	82.3(2)	O(12)-Mn(3)-O(1)	126.3(3)
				O(15)-Mn(3)-N(1)	70.6(2)	O(7)-Mn(3)-O(13)	95.0(2)
				O(10)-Mn(3)-N(1)	95.5(3)	O(15)-Mn(3)-O(13)	137.6(2)
				O(7)-Mn(3)-O(12)	86.3(3)	O(10)-Mn(3)-O(13)	81.9(3)
				O(15)-Mn(3)-O(12)	162.9(3)	N(1)-Mn(3)-O(13)	150.8(3)
				O(10)-Mn(3)-O(12)	84.1(3)	O(12)-Mn(3)-O(13)	54.3(3)
				N(1)-Mn(3)-O(12)	96.5(3)	O(1)-Mn(3)-O(13)	73.5(2)

mechanism involving the reduction of Mn_3O and fragmentation and recombination steps. Complexes **3** and **4** are highly soluble in solvents, such as CH_2Cl_2, acetone, MeCN, tetrahydrofuran, MeOH, EtOH, and N,N-dimethylformamide.

Table 3. Bond Valence Sums of Mn Atoms in Complexes **1** and **2**

	complex **1**				complex **2**			
	Mn(**1**)	Mn(**2**)	Mn(**3**)	Mn(**4**)	Mn(**1**)	Mn(**2**)	Mn(**3**)	Mn(**4**)
Mn(II)	2.935	3.514	***2.011***	***2.102***	2.906	3.514	***1.940***	***2.223***
Mn(III)	***3.045***	***3.241***	1.854	1.938	***3.013***	***3.240***	1.789	2.050
Mn(IV)	2.988	3.180	1.820	1.902	2.957	3.059	1.756	2.011

Scheme 1

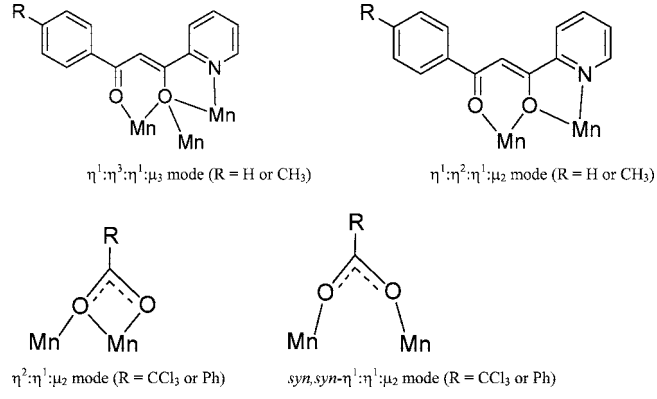

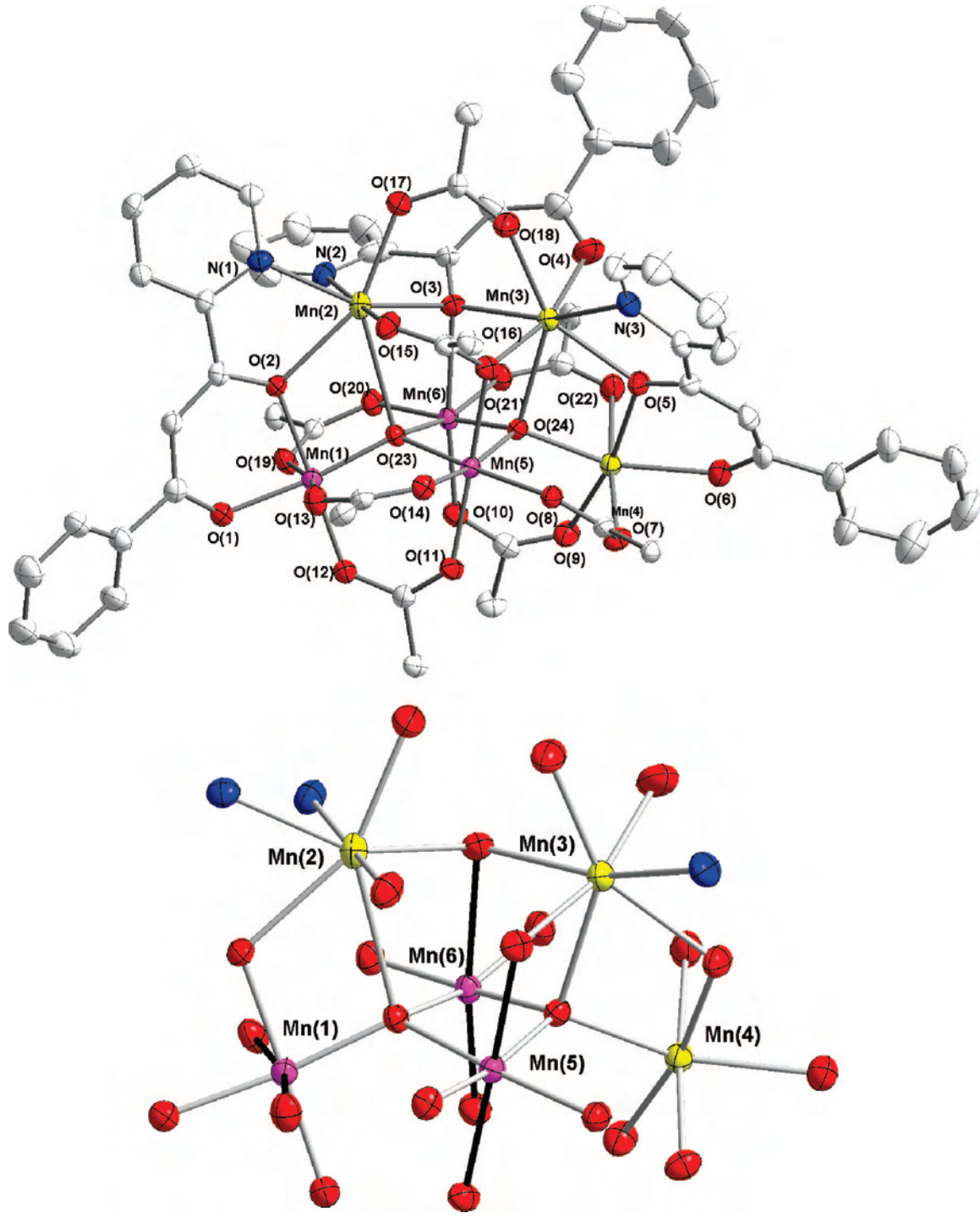

Figure 3. ORTEP drawings of **3** (top) and the JT axes orientation (highlight bond) in core the structure (bottom) with thermal ellipsoids set at 30% probability. The benzoate rings, H atoms, and solvated molecules have been omitted for clarity.

Description of Structure. $[Mn_4O(O_2CCCl_3)_6(L^1)_2]\cdot 2CH_2Cl_2$ ($1\cdot 2CH_2Cl_2$) and $[Mn_4O(O_2CCCl_3)_6(L^2)_2]\cdot 2CH_2Cl_2\cdot H_2O$ ($2\cdot 2CH_2Cl_2\cdot H_2O$). Crystallographic data of complexes $1\cdot 2CH_2Cl_2$, $2\cdot 2CH_2Cl_2\cdot H_2O$, $3\cdot 1.5CH_2Cl_2\cdot Et_2O\cdot H_2O$, and $4\cdot 2CH_2Cl_2$ are summarized in Table 1. For complexes **1** and **2**, ORTEP representations are shown in Figures 1 and 2, respectively, and selected interatomic distances and angles are listed in Table 2. Complex $1\cdot 2CH_2Cl_2$ crystallizes in triclinic space group $P\bar{1}$ with the molecule in a general position, and the asymmetric unit contains the whole cluster and two CH_2Cl_2. The central $[Mn_4(\mu_4\text{-}O)]^{8+}$ core can be described as a distorted Mn_4 tetrahedron with two Mn^{III} ions and two Mn^{II} ions in octahedral environments. A μ_4-O atom bridges the four manganese ions. The molecule of **1** does not have any crystallographic symmetry, and all of the Mn centers possess a distorted octahedral geometry. The bond valence sum (BVS) calculations (Table 3) agree with a valence-trapped description of Mn(3) and Mn(4) being Mn^{II} and Mn(1) and Mn(2) being Mn^{III}. The Mn^{III} centers are six-coordinated

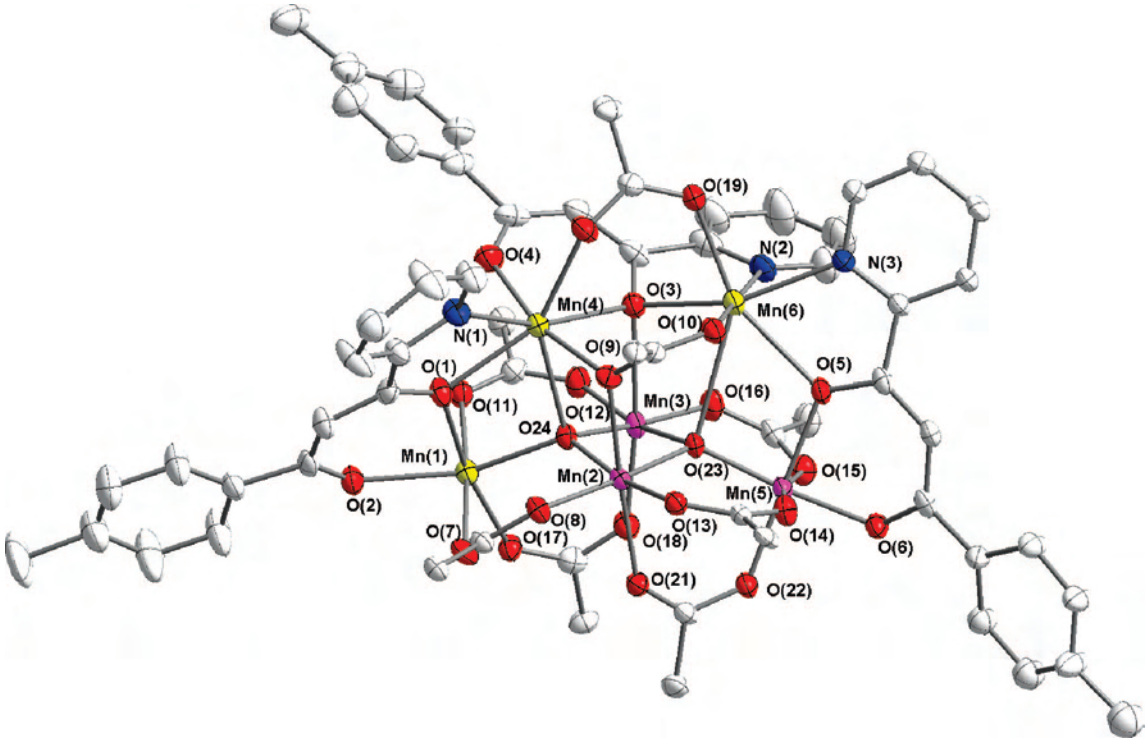

Figure 4. ORTEP drawing of **4** with thermal ellipsoids set at 30% probability. The benzoate rings, H atoms, and solvated molecules have been omitted for clarity.

Mn(1) and Mn(2), each of them clearly possessing a JT distortion in the form of axis elongation along the O(6)−Mn(1)−O(16) and O(9)−Mn(2)−O(15) axes. The JT axes at the two Mn^{III} ions in the complex are nearly perpendicular. As expected, the JT axes are located so as to avoid Mn−O^{2-} bonds, which are the shortest and strongest in the molecule (<1.9 Å). The Mn−Mn separations fall in the range of 3.214−3.674 Å, with shortest one being between $Mn^{III}Mn^{II}$ ions Mn(1) and Mn(4), which are bridged through the μ_4-O atom and O(2) of the diketonae group, and the longest one being between the Mn^{II} ions Mn(3) and Mn(4), which are bridged only by the μ_4-O atom and two bidentate chelate carboxylato ligands. The angles around the (μ_4-O)Mn_4 center vary from 98.8(2) to 120.2(3)°, consistent with a distorted tetrahedral geometry and an μ_4-O^{2-} ion rather than a square-pyramidal geometry, which is expected for a μ_4-OH group and for which the Mn atoms should have a square-planar arrangement. The peripheral ligations in complex are provided by six bridging trichloroacetate groups and two bridging diketonate groups. These two diketonate ligands behave as η^1:η^2:η^1:μ_2 ligands; each ligand chelates one metal ion through its nitrogen atoms [N(1) and N(2)] and connects this metal ion with a second one through bridging O atoms [O(2) and O(4)]. The two η^1:η^2:η^1:μ_2 diketone ligands each bridge one Mn^{III} and one Mn^{II} ion, in which O(2) and O(4) are bridging atoms and N(1) and N(2) and O(3) and O(5) are terminal atoms. The six bridging $Cl_3CCO_2^-$ groups can be separated into three classes: the groups bearing O(6)−O(9) each bridge two Mn^{III} ions while the groups bearing O(10)−O(13) each bridge two Mn^{II} ions, and the groups bearing O(14)−O(17) each bridge one Mn^{II} and one Mn^{III} ion.

The structure of complex **2** is very similar to that of **1** except that one of six $Cl_3CCO_2^-$groups is bridging two Mn's in a η^2:η^1:μ_2 binding mode, completing a distorted pentagonal bipyramid coordination environment around Mn(3). The coordination modes of diketonate ligands and trichloroacetate are shown in Scheme 1.

The structures of complexes **1** and **2** are two new examples of Mn_4 clusters with the tetrahedron [Mn_4(μ_4-O)] core, and the other structurally characterized members of this family are [$Mn^{II}_2Mn^{III}_2$O(L)$(OAc)_3$Cl(MeOH)], [$Mn^{II}_2Mn^{III}_2$O(L)$(OAc)_4(H_2O)$] (L = tetra-anion macrocyclic [2 + 2] Schiff-base ligand),[35] [Mn^{III}_4O$(salen)_4$(Na-diglyme$)_2$] (salen = *N*,*N*′-*o*-ethylenebis(salicylideneiminato) dianion; diglyme = diethylene glycol dimethyl ether),[36] [Mn^{II}_4O(DPHF)] (DPHF = *N*,*N*′-diphenylformamidinate),[37] [$Mn^{II}_4I_6O(PPr_3)_4$],[38] and [$Mn^{II}_3Mn^{IV}$O$(pko)_4$(3,4-D$)_4$] (pko = di(2-pyridyl)keton-oxime; 3,4-D = 3,4-dichlorophenoxy acetic acid).[39]

$[Mn_6O_2(O_2CPh)_8(L^1)_3]\cdot 1.5CH_2Cl_2\cdot Et_2O\cdot H_2O$ ($3\cdot 1.5CH_2Cl_2\cdot Et_2O\cdot H_2O$) and $[Mn_6O_2(O_2CPh)_8(L^2)_3]\cdot 2CH_2Cl_2$ ($4\cdot 2CH_2Cl_2$). Both complexes $3\cdot 1.5CH_2Cl_2\cdot Et_2O\cdot H_2O$ and $4\cdot 2CH_2Cl_2$ are crystallized in the monoclinic space group $P2_1/n$. The ORTEP representations of **3** and **4** are shown in Figures 3 and 4, respectively, and selected interatomic

(35) (a) McKee, V.; Tandon, S. S. *J. Chem. Soc., Chem. Commun.* **1988**, 1334. (b) McCrea, J.; McKee, V.; Metcalfe, T.; Tandon, S. S.; Wikaira, J. *Inorg. Chim. Acta* **2000**, *297*, 220.
(36) Gallo, E.; Solari, E.; Angelis, S.; Floriani, C.; Re, N.; Chiesi-Villa, A.; Rizzoli, C. *J. Am. Chem. Soc.* **1993**, *115*, 9850.
(37) Cotton, F. A.; Daniels, L. M.; Falvello, L. R.; Matonic, J. H.; Murillo, C. A.; Wang, X.; Zhou, H. *Inorg. Chim. Acta* **1997**, *266*, 91.
(38) Beagley, B.; McAuliffe, C. A.; Mac Rory, P. P.; Ndifon, P. T.; Pritchard, R. G. *J. Chem. Soc., Chem. Commun.* **1990**, 309.
(39) Afrati, T.; Dendrinou-Samara, C.; Raptopoulou, C. P.; Terzis, A.; Tangoulis, V.; Kessissoglou, D. P. *Angew. Chem., Int. Ed.* **2002**, *41*, 2148.

Table 4. Selected Bond Distances (Å) and Angles (deg) for Complexes **3**·1.5CH_2Cl_2·Et_2O·H_2O and **4**·2CH_2Cl_2

	3·1.5CH_2Cl_2·Et_2O·H_2O				**4**·2CH_2Cl_2		
Mn(1)-O(23)	1.881(4)	Mn(4)-O(9)	2.139(5)	Mn(1)-O(17)	2.117(5)	Mn(4)-O(9)	2.153(5)
Mn(1)-O(1)	1.938(4)	Mn(4)-O(24)	2.150(4)	Mn(1)-O(24)	2.152(4)	Mn(4)-O(20)	2.209(5)
Mn(1)-O(2)	2.040(4)	Mn(4)-O(6)	2.179(5)	Mn(1)-O(11)	2.164(5)	Mn(4)-O(1)	2.255(4)
Mn(1)-O(19)	2.110(4)	Mn(4)-O(7)	2.185(4)	Mn(1)-O(2)	2.178(4)	Mn(4)-N(1)	2.346(6)
Mn(1)-O(13)	2.115(5)	Mn(4)-O(5)	2.217(4)	Mn(1)-O(1)	2.187(5)	Mn(4)-O(3)	2.376(4)
Mn(2)-O(15)	2.115(5)	Mn(5)-O(24)	1.877(4)	Mn(1)-O(7)	2.202(5)	Mn(4)-O(24)	2.414(5)
Mn(2)-O(17)	2.186(5)	Mn(5)-O(23)	1.920(4)	Mn(2)-O(24)	1.886(4)	Mn(5)-O(23)	1.861(4)
Mn(2)-N(2)	2.256(6)	Mn(5)-O(8)	1.959(4)	Mn(2)-O(23)	1.920(4)	Mn(5)-O(6)	1.927(4)
Mn(2)-N(1)	2.289(5)	Mn(5)-O(14)	1.992(4)	Mn(2)-O(8)	1.951(4)	Mn(5)-O(22)	1.994(4)
Mn(2)-O(2)	2.310(4)	Mn(5)-O(11)	2.136(4)	Mn(2)-O(13)	2.006(4)	Mn(5)-O(5)	2.032(4)
Mn(2)-O(3)	2.328(4)	Mn(5)-O(16)	2.242(4)	Mn(2)-O(21)	2.126(5)	Mn(5)-O(14)	2.108(5)
Mn(3)-O(4)	2.139(6)	Mn(6)-O(24)	1.841(4)	Mn(2)-O(9)	2.212(4)	Mn(5)-O(15)	2.116(5)
Mn(3)-O(16)	2.159(5)	Mn(6)-O(20)	1.938(4)	Mn(3)-O(24)	1.846(4)	Mn(6)-O(10)	2.111(5)
Mn(3)-O(5)	2.228(4)	Mn(6)-O(23)	1.949(4)	Mn(3)-O(23)	1.928(4)	Mn(6)-O(19)	2.172(5)
Mn(3)-O(18)	2.238(5)	Mn(6)-O(21)	1.969(4)	Mn(3) O(16)	1.946(4)	Mn(6)-N(2)	2.259(6)
Mn(3)-O(3)	2.329(4)	Mn(6)-O(10)	2.092(4)	Mn(3)-O(12)	1.948(5)	Mn(6)-N(3)	2.294(5)
Mn(3)-N(3)	2.361(6)	Mn(6)-O(3)	2.395(4)	Mn(3)-O(18)	2.120(5)	Mn(6)-O(3)	2.304(4)
Mn(3)-O(24)	2.451(4)			Mn(3)-O(3)	2.420(5)	Mn(6)-O(5)	2.365(5)
				Mn(4)-O(4)	2.090(5)		
O(23)-Mn(1)-O(1)	172.60(18)	O(8)-Mn(5)-O(16)	85.60(16)				
O(23)-Mn(1)-O(12)	96.84(17)	O(14)-Mn(5)-O(16)	81.78(17)	O(17)-Mn(1)-O(24)	95.75(17)	O(23)-Mn(5)-O(6)	174.21(19)
O(1)-Mn(1)-O(12)	89.94(18)	O(11)-Mn(5)-O(16)	169.98(17)	O(17)-Mn(1)-O(11)	91.50(19)	O(23)-Mn(5)-O(22)	95.93(17)
O(23)-Mn(1)-O(2)	84.38(17)	O(24)-Mn(5)-Mn(6)	39.60(12)	O(24)-Mn(1)-O(11)	95.40(16)	O(6)-Mn(5)-O(22)	89.10(18)
O(1)-Mn(1)-O(2)	88.74(17)	O(23)-Mn(5)-Mn(6)	43.04(12)	O(17)-Mn(1)-O(2)	109.26(18)	O(23)-Mn(5)-O(5)	85.29(17)
O(12)-Mn(1)-O(2)	177.58(18)	O(8)-Mn(5)-Mn(6)	132.64(13)	O(24)-Mn(1)-O(2)	154.46(19)	O(6)-Mn(5)-O(5)	89.59(17)
O(23)-Mn(1)-O(19)	95.78(17)	O(14)-Mn(5)-Mn(6)	142.10(13)	O(11)-Mn(1)-O(2)	89.21(17)	O(22)-Mn(5)-O(5)	177.8(2)
O(1)-Mn(1)-O(19)	86.96(18)	O(11)-Mn(5)-Mn(6)	91.33(12)	O(17)-Mn(1)-O(1)	169.89(17)	O(23)-Mn(5)-O(14)	95.61(19)
O(12)-Mn(1)-O(19)	91.63(18)	O(16)-Mn(5)-Mn(6)	98.15(11)	O(24)-Mn(1)-O(1)	74.25(16)	O(6)-Mn(5)-O(14)	81.44(19)
O(2)-Mn(1)-O(19)	90.33(18)	O(24)-Mn(6)-O(20)	175.95(19)	O(11)-Mn(1)-O(1)	90.94(18)	O(22)-Mn(5)-O(14)	90.62(19)
O(23)-Mn(1)-O(13)	95.60(17)	O(24)-Mn(6)-O(23)	81.09(17)	O(2)-Mn(1)-O(1)	80.58(17)	O(5)-Mn(5)-O(14)	87.47(19)
O(1)-Mn(1)-O(13)	81.29(18)	O(20)-Mn(6)-O(23)	96.41(17)	O(17)-Mn(1)-O(7)	89.87(19)	O(23)-Mn(5)-O(15)	96.27(19)
O(12)-Mn(1)-O(13)	90.81(19)	O(24)-Mn(6)-O(21)	97.61(18)	O(24)-Mn(1)-O(7)	88.17(16)	O(6)-Mn(5)-O(15)	86.4(2)
O(2)-Mn(1)-O(13)	86.99(18)	O(20)-Mn(6)-O(21)	83.99(18)	O(11)-Mn(1)-O(7)	176.03(16)	O(22)-Mn(5)-O(15)	91.7(2)
O(19)-Mn(1)-O(13)	167.99(18)	O(23)-Mn(6)-O(21)	165.23(18)	O(2)-Mn(1)-O(7)	86.82(18)	O(5)-Mn(5)-O(15)	89.92(19)
O(15)-Mn(2)-O(17)	86.71(19)	O(24)-Mn(6)-O(10)	96.52(18)	O(1)-Mn(1)-O(7)	88.35(18)	O(14)-Mn(5)-O(15)	167.59(18)
O(15)-Mn(2)-N(2)	174.14(19)	O(20)-Mn(6)-O(10)	87.14(18)	O(24)-Mn(2)-O(23)	80.25(17)	O(10)-Mn(6)-O(19)	88.9(2)
O(17)-Mn(2)-N(2)	90.0(2)	O(23)-Mn(6)-O(10)	102.95(18)	O(24)-Mn(2)-O(8)	94.69(18)	O(10)-Mn(6)-N(2)	176.0(2)
O(15)-Mn(2)-N(1)	90.36(18)	O(21)-Mn(6)-O(10)	91.83(19)	O(23)-Mn(2)-O(8)	174.94(19)	O(19)-Mn(6)-N(2)	90.1(2)
O(17)-Mn(2)-N(1)	84.58(18)	O(24)-Mn(6)-O(3)	81.42(16)	O(24)-Mn(2)-O(13)	167.56(19)	O(10)-Mn(6)-N(3)	91.02(19)
N(2)-Mn(2)-N(1)	84.5(2)	O(20)-Mn(6)-O(3)	95.18(17)	O(23)-Mn(2)-O(13)	99.82(17)	O(19)-Mn(6)-N(3)	87.38(18)
O(15)-Mn(2)-O(2)	94.58(17)	O(23)-Mn(6)-O(3)	83.88(16)	O(8)-Mn(2)-O(13)	85.11(17)	N(2)-Mn(6)-N(3)	85.0(2)
O(17)-Mn(2)-O(2)	153.90(16)	O(21)-Mn(6)-O(3)	81.38(17)	O(24)-Mn(2)-O(21)	105.10(19)	O(10)-Mn(6)-O(3)	112.17(16)
N(2)-Mn(2)-O(2)	86.22(19)	O(10)-Mn(6)-O(3)	172.54(17)	O(23)-Mn(2)-O(21)	91.12(17)	O(19)-Mn(6)-O(3)	80.80(17)
N(1)-Mn(2)-O(2)	69.37(16)	O(24)-Mn(6)-Mn(5)	40.53(13)	O(8)-Mn(2)-O(21)	90.20(18)	N(2)-Mn(6)-O(3)	71.49(19)
O(15)-Mn(2)-O(3)	111.67(17)	O(20)-Mn(6)-Mn(5)	137.71(13)	O(13)-Mn(2)-O(21)	87.34(18)	N(3)-Mn(6)-O(3)	153.55(19)
O(17)-Mn(2)-O(3)	79.06(17)	O(23)-Mn(6)-Mn(5)	42.25(11)	O(24)-Mn(2)-O(9)	85.65(18)	O(10)-Mn(6)-O(5)	92.53(17)
N(2)-Mn(2)-O(3)	72.39(18)	O(21)-Mn(6)-Mn(5)	138.13(13)	O(23)-Mn(2)-O(9)	93.70(17)	O(19)-Mn(6)-O(5)	155.92(15)
N(1)-Mn(2)-O(3)	151.45(18)	O(10)-Mn(6)-Mn(5)	93.67(13)	O(8)-Mn(2)-O(9)	85.87(17)	N(2)-Mn(6)-O(5)	86.8(2)
O(2)-Mn(2)-O(3)	123.84(15)	O(3)-Mn(6)-Mn(5)	89.40(11)	O(13)-Mn(2)-O(9)	81.93(17)	N(3)-Mn(6)-O(5)	68.57(17)
O(4)-Mn(3)-O(16)	164.6(2)	C(14)-N(1)-Mn(2)	122.8(4)	O(21)-Mn(2)-O(9)	168.85(18)	O(3)-Mn(6)-O(5)	120.45(16)
O(4)-Mn(3)-O(5)	87.0(2)	O(3)-Mn(3)-O(24)	71.50(14)	O(24)-Mn(2)-Mn(3)	39.62(12)	O(12)-Mn(3)-Mn(2)	139.04(14)
O(16)-Mn(3)-O(5)	108.39(17)	N(3)-Mn(3)-O(24)	124.40(18)	O(23)-Mn(2)-Mn(3)	42.25(13)	O(18)-Mn(3)-Mn(2)	93.83(14)
O(4)-Mn(3)-O(18)	83.2(2)	O(9)-Mn(4)-O(24)	96.43(17)	O(8)-Mn(2)-Mn(3)	132.82(13)	O(3)-Mn(3)-Mn(2)	90.24(11)
O(16)-Mn(3)-O(18)	83.55(19)	O(9)-Mn(4)-O(22)	89.39(19)	O(13)-Mn(2)-Mn(3)	142.07(12)	O(4)-Mn(4)-O(9)	166.36(18)
O(5)-Mn(3)-O(18)	147.60(17)	O(24)-Mn(4)-O(22)	93.94(17)	O(21)-Mn(2)-Mn(3)	92.08(13)	O(4)-Mn(4)-O(20)	86.7(2)
O(4)-Mn(3)-O(3)	80.9(2)	O(9)-Mn(4)-O(6)	109.49(18)	O(9)-Mn(2)-Mn(3)	98.26(12)	O(9)-Mn(4)-O(20)	82.45(18)
O(16)-Mn(3)-O(3)	89.07(16)	O(24)-Mn(4)-O(6)	153.65(17)	O(24)-Mn(3)-O(23)	81.03(18)	O(4)-Mn(4)-O(1)	83.23(18)
O(5)-Mn(3)-O(3)	129.21(16)	O(22)-Mn(4)-O(6)	91.05(18)	O(24)-Mn(3)-O(16)	174.4(2)	O(9)-Mn(4)-O(1)	110.29(16)
O(18)-Mn(3)-O(3)	79.51(17)	O(9)-Mn(4)-O(7)	93.28(18)	O(23)-Mn(3)-O(16)	96.31(19)	O(20)-Mn(4)-O(1)	148.30(18)
O(4)-Mn(3)-N(3)	99.6(2)	O(24)-Mn(4)-O(7)	89.20(16)	O(24)-Mn(3)-O(12)	98.40(19)	O(4)-Mn(4)-N(1)	98.2(2)
O(16)-Mn(3)-N(3)	86.18(19)	O(22)-Mn(4)-O(7)	175.64(18)	O(23)-Mn(3)-O(12)	166.9(2)	O(9)-Mn(4)-N(1)	88.8(2)
O(5)-Mn(3)-N(3)	69.56(19)	O(6)-Mn(4)-O(7)	84.81(17)	O(16)-Mn(3)-O(12)	83.1(2)	O(20)-Mn(4)-N(1)	83.17(19)
O(18)-Mn(3)-N(3)	81.7(2)	O(9)-Mn(4)-O(5)	169.90(17)	O(24)-Mn(3)-O(18)	97.50(19)	O(1)-Mn(4)-N(1)	68.72(18)
O(3)-Mn(3)-N(3)	161.06(19)	O(24)-Mn(4)-O(5)	74.21(16)	O(23)-Mn(3)-O(18)	102.01(19)	O(4)-Mn(4)-O(3)	80.16(19)
O(4)-Mn(3)-O(24)	112.7(2)	O(22)-Mn(4)-O(5)	87.51(19)	O(16)-Mn(3)-O(18)	87.8(2)	O(9)-Mn(4)-O(3)	89.57(16)
O(16)-Mn(3)-O(24)	74.53(15)	O(6)-Mn(4)-O(5)	80.19(17)	O(12)-Mn(3)-O(18)	91.1(2)	O(20)-Mn(4)-O(3)	78.78(17)
O(5)-Mn(3)-O(24)	68.37(14)	O(7)-Mn(4)-O(5)	90.44(17)	O(24)-Mn(3)-O(3)	81.75(17)	O(1)-Mn(4)-O(3)	128.39(17)
O(18)-Mn(3)-O(24)	143.55(16)	O(24)-Mn(5)-O(23)	80.97(16)	O(23)-Mn(3)-O(3)	85.00(17)	N(1)-Mn(4)-O(3)	161.94(18)
O(24)-Mn(5)-O(8)	94.55(17)	O(23)-Mn(5)-O(11)	90.94(16)	O(16)-Mn(3)-O(3)	93.18(19)	O(4)-Mn(4)-O(24)	109.6(2)
O(23)-Mn(5)-O(8)	175.52(18)	O(8)-Mn(5)-O(11)	90.38(17)	O(12)-Mn(3)-O(3)	81.97(19)	O(9)-Mn(4)-O(24)	75.24(15)
O(24)-Mn(5)-O(14)	166.95(18)	O(14)-Mn(5)-O(11)	88.75(17)	O(18)-Mn(3)-O(3)	172.78(18)	O(20)-Mn(4)-O(24)	143.24(16)
O(23)-Mn(5)-O(14)	99.06(17)	O(24)-Mn(5)-O(16)	85.19(17)	O(24)-Mn(3)-Mn(2)	40.64(13)	O(1)-Mn(4)-O(24)	68.13(15)
O(8)-Mn(5)-O(14)	85.25(18)	O(23)-Mn(5)-O(16)	93.77(16)	O(23)-Mn(3)-Mn(2)	42.03(11)	N(1)-Mn(4)-O(24)	124.44(17)
O(24)-Mn(5)-O(11)	104.30(17)			O(16)-Mn(3)-Mn(2)	137.70(15)	O(3)-Mn(4)-O(24)	72.30(14)

distances and angles are listed in Table 4. Complexes **3** and **4** are isostructural, with similar metric parameters. The structure of **3** reveals a $[Mn^{II}_3Mn^{III}_3(\mu_4\text{-}O)_2]^{11+}$ core, which comprises a central, distorted cubanelike $[Mn^{II}_2Mn^{III}_2O_2(OR)(O_2CR)]$, to either side of which is attached one Mn^{III} [Mn(1)] and one Mn^{II} [Mn(4)] ion by two μ_4-O^{2-} ions. The

Table 5. Bond Valence Sums of Mn Atoms in Complexes **3** and **4**

	complex **3**						complex **4**					
	Mn(1)	Mn(2)	Mn(3)	Mn(4)	Mn(5)	Mn(6)	Mn(1)	Mn(2)	Mn(3)	Mn(4)	Mn(5)	Mn(6)
Mn(II)	3.373	***1.855***	***2.079***	***2.138***	3.394	3.446	***2.174***	3.403	3.449	***2.039***	3.450	***1.828***
Mn(III)	***3.110***	1.711	1.918	1.971	***3.131***	***3.178***	2.005	***3.138***	***3.180***	1.880	***3.181***	1.686
Mn(IV)	3.052	1.678	1.881	1.934	3.072	3.119	1.967	3.079	3.121	1.845	3.121	1.654

peripheral ligations were provided by eight $PhCO_2^-$groups and three diketonate ligands. Seven of eight $PhCO_2^-$groups are bridged to two Mn ions and are in their familiar *syn,syn*-η^1:η^1:μ_2 binding modes. The final one is in the fairly rare η^1:η^2:μ_3 mode, O(15) terminal to Mn(2) and O(16) bridging Mn(3) and Mn(5). The three L^- groups are categorized into two groups: (i) Two behave as η^1:η^2:η^1:μ_2 ligands; each ligand chelates one metal ion through its nitrogen atom [N(1) and N(3)] and connects this metal ion with a second one through a bridging O atom [O(2) and O(5)] and one terminal O atom [O(1) and O(6)]. (ii) One chelates in the η^1:η^3:η^1:μ_3 bridging type; the coordination of this ligand is similar to that in i for terminal N(2) and O(4) atoms but bridging three Mn ions in O(3). For complex **3**, Mn(1), Mn(4), Mn(5), and Mn(6) are six-coordinate with slightly distorted octahedral geometries, while Mn(2) and Mn(3) are seven-coordinate with distorted pentagonal bipyramidal geometries. In addition, although a weak interaction in Mn(2)−O(23) at a distance of 2.751(3), it was considered as the seventh coordination position around Mn(2). Charge considerations require a $3Mn^{II}/3Mn^{III}$ oxidation state description, and Mn(2), Mn(3), and Mn(4) are assigned as the Mn^{II} ions on the basis of (i) the longer average bond lengths at these ions compared with those of the other Mn ions, (ii) the clear presence of the JT axial elongation at Mn(1), Mn(5), and Mn(6), as expected for a high-spin d^4 ion in near-octahedral geometry, and (iii) BVS calculations which give values (Table 5) in good agreement with the above assignments. In addition, an intermolecular π-stacking interaction was only shown in complex **3**; one L^- ligand [N(1), C(10)−C(14)] interacts with one phenyl ring of the benzoate [C(44)−C(49)] with a ring separation of ~3.8 Å, as shown in Figure 5.

Complexes **3** and **4** possess a structure that is quite different from that of any previously structurally characterized hexanuclear Mn−carboxylate complexes. These complexes are $[Mn_6O_2(O_2CR)_{10}L_4]$ (R = Ph, CMe_3, CCl_3; L = H_2O, py, MeCN),[40] $[Mn_6O_2(O_2CPh)_{12}(py)_2]$,[41] $[Mn_6O_8(mpdp)_3(bpy)_3](ClO_4)$ (mpdp = *m*-phenylenedipropionate),[42] $[Mn_6O_2(O_2CR)_2(salox)_6(EtOH)_4]$ (R = CMe, Ph),[43] $[Mn_6O_2(O_2CPh)_{10}(S)_4]$ (S = py, MeCN, DMF),[44] $[Mn_6O_2(O_2CH_2)(O_2CPet)_{11}(HO_2CPet)_2(O_2CMe)_2]$,[45] $[Mn_6O_4(O_2CMe)_2(O_2Ac)_4(Mesalim)_4]$,[46] $[Mn_6O_2(Etsao)_6(O_2CCMe_3)_2(EtOH)_5]$,[47] and $[Mn_6O_2(Etsao)_6(O_2CPh(Me)_2)_2(EtOH)_6]$.[48]

Magnetic Properties of Complexes 1 and 2. The temperature dependences of the DC magnetic susceptibilities for **1** and **2** measured in the temperature range of 2.0–300 K in a 1.0 kG magnetic field are illustrated in Figure 6. The value of $\chi_M T$ steadily decreases from 13.51 emu K mol^{-1} for **1** and 14.18 emu K mol^{-1} for **2** at 300 K to 0.31 emu K mol^{-1} for **1** and 0.43 emu K mol^{-1} for **2** at 2.0 K. The values at 300 K are slightly less than the calculated spin-only value of 14.75 at emu K mol^{-1} for a $Mn^{II}_2Mn^{III}_2$ complex with noninteracting metal centers with $g = 2.0$, suggesting antiferromagnetic interactions. The monotonically decreasing $\chi_M T$ with temperature and the resultant low values of $\chi_M T$ at 2.0 K are indicative of a small ground state for compounds **1** and **2**. A consideration of the topologies of the complexes affords the coupling scheme depicted in Figure 7. On the basis of the nature of the Mn−O−Mn bonds, the six coupling constants that are strictly required can be reduced to three, where J_1, J_2, and J_3 characterize the coupling between Mn^{II}−Mn^{III}, Mn^{II}−Mn^{II}, and Mn^{III}−Mn^{III} through μ_4-O, respectively. The spin Hamiltonian is given in eq 3. The equivalent spin Hamiltonian in eq 4 is obtained by applying the Kambe coupling approach (eq 5) where only three dominant exchange pathways are considered (Figure 4). The $\chi_M T$ versus temperature results for both complexes were least-squares-fit to the van Vleck equation, with a theoretical χ_M versus T equation being derived (see the Supporting Information), which includes the eigenvalue expression in eq 6.

$$H = -2J_1(S_1S_3 + S_1S_4 + S_2S_3 + S_2S_4) - 2J_2(S_3S_4) - 2J_3(S_1S_2) \quad (3)$$

$$H = -J_1(\hat{S}_T^2 - \hat{S}_A^2 - \hat{S}_B^2) - J_2(\hat{S}_B^2) - J_3(\hat{S}_A^2) \quad (4)$$

where

$$\hat{S}_A = \hat{S}_1 + \hat{S}_2;\ \hat{S}_B = \hat{S}_3 + \hat{S}_4;\ \text{and}\ \hat{S}_T = \hat{S}_A + \hat{S}_B \quad (5)$$

The Kambe equivalent operator method gives the eigenvalue expression in eq 6.

(40) (a) Murrie, M.; Parsons, S.; Winpenny, R. E. P. *Dalton Trans.* **1998**, 1423. (b) Stamatatos, T. C.; Foguet-Albiol, D.; Perlepes, S. P.; Raptopoulou, C. P.; Terzis, A.; Patrickios, C. S.; Christou, G.; Tasiopoulos, A. J. *Polyhedron* **2006**, *25*, 1737.

(41) Low, D. M.; Brechin, E. K.; Helliwell, M.; Mallah, T.; Rivière, E.; McInnes, E. J. L. *Chem. Commun.* **2003**, 2330.

(42) Cañada-Vilalta, C.; Streib, W. E.; Huffman, J. C.; O'Brien, T. A.; Davidson, E. R.; Christou, G. *Inorg. Chem.* **2004**, *43*, 101.

(43) Milios, C. J.; Raptopoulou, C. P.; Terzis, A.; Lloret, F.; Vicente, R.; Perlepes, S. P.; Escuer, A. *Angew. Chem., Int. Ed.* **2004**, *43*, 210.

(44) (a) Schake, A. R.; Vincent, J. B.; Li, Q.; Boyd, P. D. W.; Folting, K.; Huffman, J. C.; Hendrickson, D. N.; Christou, G. *Inorg. Chem.* **1989**, *28*, 1915. (b) Gavrilenko, K. S.; Punin, S. V.; Cador, O.; Golhen, S.; Ouahab, L.; Pavlishchuk, V. V. *Inorg. Chem.* **2005**, *44*, 5903.

(45) Chakov, N. E.; Zakharov, L. N.; Rheingold, A. L.; Abboud, K. A.; Christou, G. *Inorg. Chem.* **2005**, *44*, 4555.

(46) Godbole, M. D.; Roubeau, O.; Mills, A. M.; Kooijman, H.; Spek, A. L.; Bouwman, E. *Inorg. Chem.* **2006**, *45*, 6713.

(47) Milios, C. J.; Vinslava, A.; Wernsdorfer, W.; Moggach, S.; Parsons, S.; Perlepes, S. P.; Christou, G.; Brechin, E. K. *J. Am. Chem. Soc.* **2007**, *129*, 9.

(48) Milios, C. J.; Vinslava, A.; Wood, P. A.; Parsons, S.; Wernsdorfer, W.; Christou, G.; Perlepes, S. P.; Brechin, E. K. *J. Am. Chem. Soc.* **2007**, *129*, 2754.

$$E(S_T) = -J_1[S_T(S_T + 1) - S_A(S_A + 1) - S_B(S_B + 1)] - J_2[(S_B(S_B + 1)] - J_3[(S_A(S_A + 1)] \quad (6)$$

With two $S = 2$ and two $S = {}^5/_2$ interacting ions, there are a total of 110 possible states with S_T, the total spin of a Mn_4 cluster, ranging from 0 to 9. The data below 10 K were omitted in the fitting, because zero-field splitting and the Zeeman effect are likely to have an effect on the susceptibilities in this temperature range. The results of fitting the experimental data are shown as solid lines in Figure 4, with final parameters being $g = 1.97$, $J_1 = -2.67$ cm^{-1}, $J_2 =$

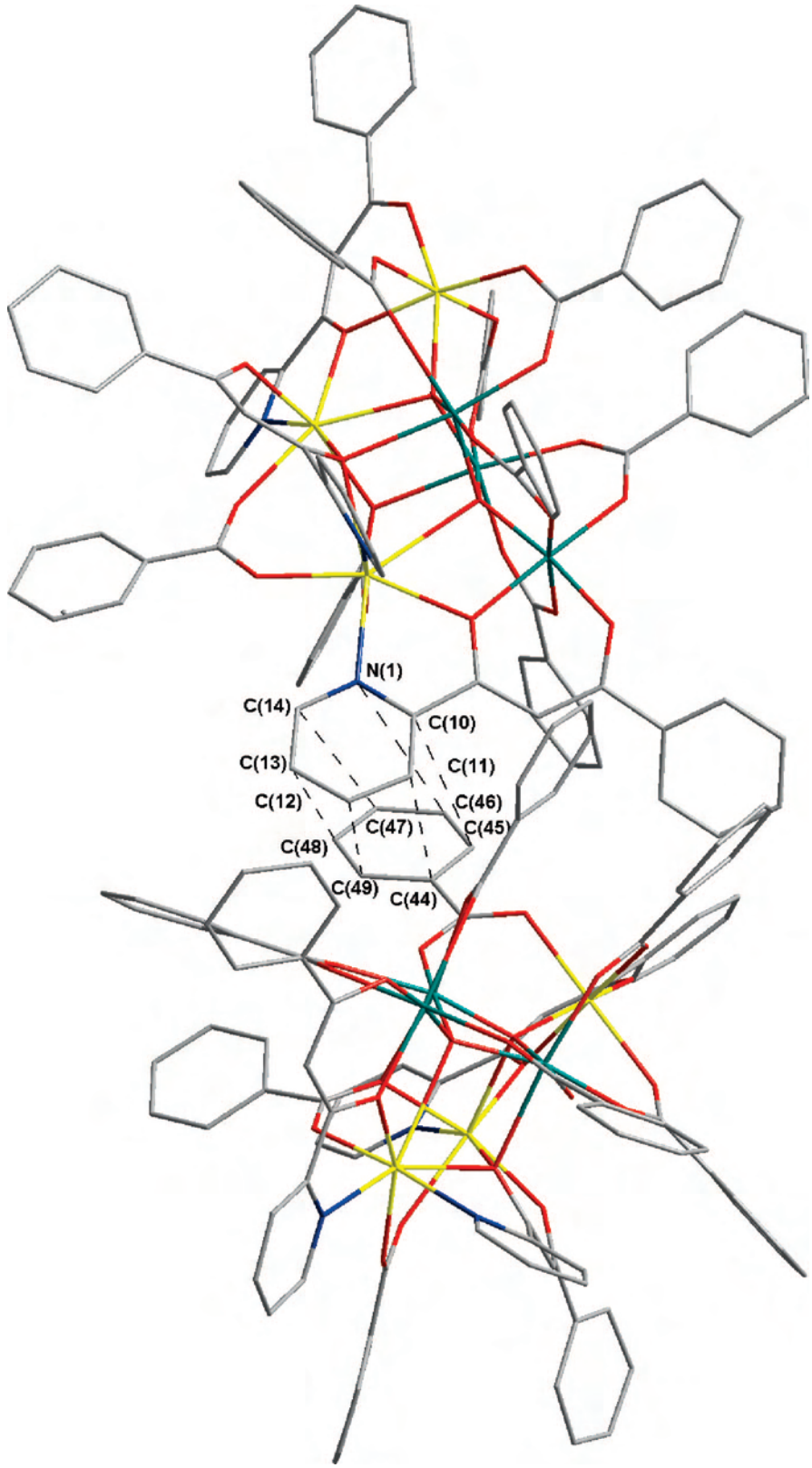

Figure 5. Intermolecular π-stacking interaction of complex **4**, one L^- ligand [N(1), C(10)−C(14)] with one phenyl ring of the benzoate [C(44)−C(49)] at a separation of ∼3.8 Å.

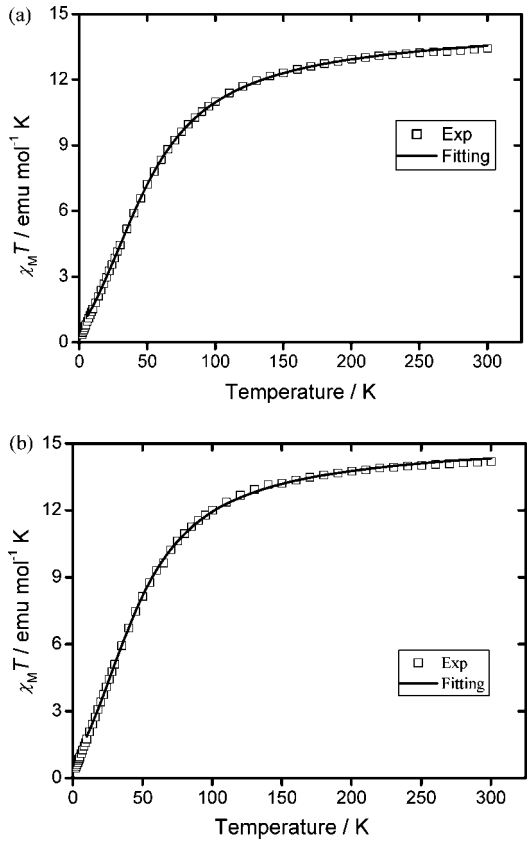

Figure 6. Plots of $\chi_M T$ vs temperature for microcrystalline samples of complexes (a) **1** and (b) **2**. The solid lines represent a least-squares fit of the data in the region 10–300 K to the van Vleck equation.

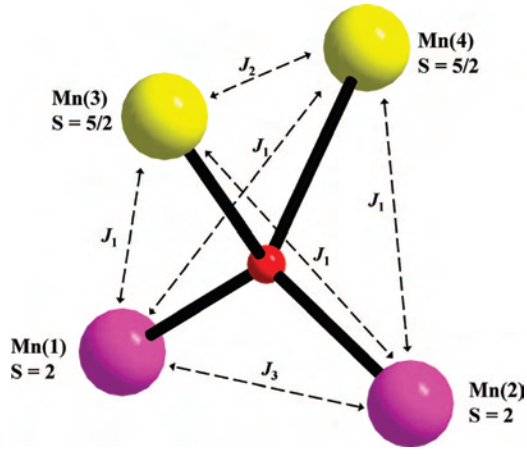

Figure 7. Diagram showing the definition of atom number and magnetic exchange parameters for the complexes (**1** and **2**) studied.

3.21 cm^{-1}, and $J_3 = 1.08$ cm^{-1} for complex **1** and $g = 2.01$, $J_1 = -2.44$ cm^{-1}, $J_2 = 3.41$ cm^{-1}, and $J_3 = 1.04$ cm^{-1} for complex **2**. In both cases, the temperature-independent paramagnetism was holding constant at 800 $\times$ 10^{-6} emu mol^{-1}. Each set of parameters results in a ground state of $S = 1$ for two complexes. The fits indicate that the Mn_4 complexes **1** and **2** have $S_T = 1$ ground states. In the notation (S_T, S_A, S_B), this is the (1, 4, 5) state in which two Mn^{III} are aligned antiparallel to Mn^{II} spins. The first excited state is the $S_T = 2$ state comprising the (2, 4, 5) states at 11 and 9 cm^{-1} above the ground state for **1**and **2**, respectively.

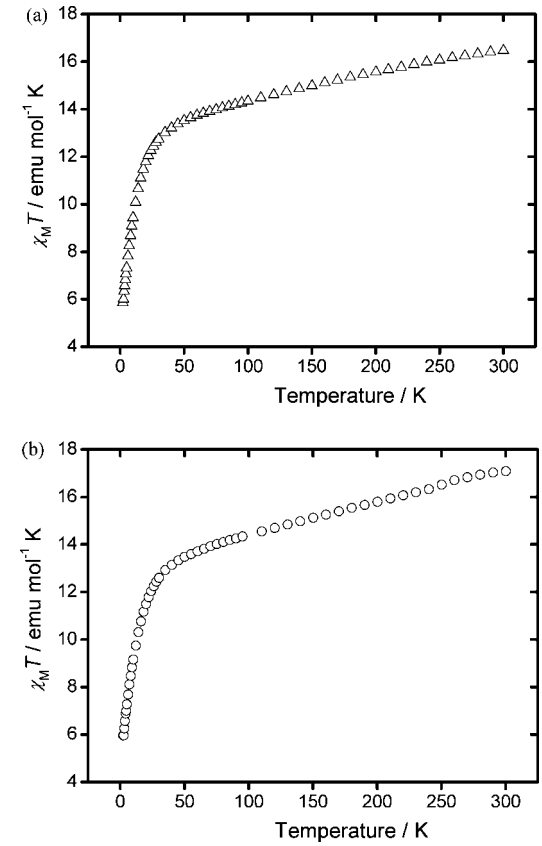

Figure 8. Plots of $\chi_M T$ vs temperature for microcrystalline samples of complexes (a) **3**·H_2O and (b) **4**.

The values obtained for exchange parameters of the two complexes are very similar. The interactions in Mn^{II}−Mn^{III}, J_1, in complexes **1** and **2** are comparable to a similar pathway in the complexes of $[Mn^{II}_4Mn^{III}_2O_2(O_2CPh)_{10}(S)_4]$ (S = py, MeCN, DMF).[44] Exchange coupling between Mn^{II} and Mn^{III} ions in these compounds is antiferromagnetic with values of −0.8 and −4.2 cm^{-1}, which close the values −2.67 and 2.44 cm^{-1} for these interactions in **1** and **2**, respectively. The interactions of J_2 (Mn^{II}−Mn^{II}) in complexes **1** and **2** are ferromagnetic with values of 3.21 and 3.41 cm^{-1}, respectively. These interactions may be due to the small angles of Mn^{II}−O−Mn^{II} (98.8 and 92.2° for **1** and **2**, respectively); these fitting results are consistent with previously reported compounds containing the $[Mn^{II}(\mu_4\text{-O})Mn^{II}]^{2+}$ unit.[49] The Mn^{III}−Mn^{III} exchange interactions in complexes **1** and **2** are consistent with the previously recognized fact that the exchange interaction is known to be very weak in complexes with the $[Mn^{III}_2O(O_2CR)_2]$ core.[50] In these complexes, the couplings between Mn^{III} ions are always small with values ranging from +9 to −5.1 cm^{-1}, and the values of 1.08 and

(49) Milios, C. J.; Piligkos, S.; Bell, A. R.; Laye, R. H.; Teat, S. J.; Vicente, R.; McInnes, E.; Escuer, A.; Perlepes, S. P.; Winpenny, R. E. P. *Inorg. Chem. Commun.* **2006**, *9*, 638.
(50) (a) Corbella, M.; Costa, R.; Ribas, J.; Fries, P. H.; Latour, J.-M.; Ohrstrom, L.; Solans, X.; Rodriguez, V. *Inorg. Chem.* **1996**, *35*, 1857. (b) Hotzelmann, R.; Wieghardt, K.; Floerke, U.; Haupt, H. J.; Weatherburn, D. C.; Bonvoisin, J.; Blondin, G.; Girerd, J. J. *J. Am. Chem. Soc.* **1992**, *114*, 1681. (c) Hendrickson, D. N.; Christou, G.; Schmitt, E. A.; Libby, E.; Bashkin, J. S.; Wang, S.; Tsai, H. L.; Vincent, J. B.; Boyd, P. D. W. *J. Am. Chem. Soc.* **1992**, *114*, 2455.

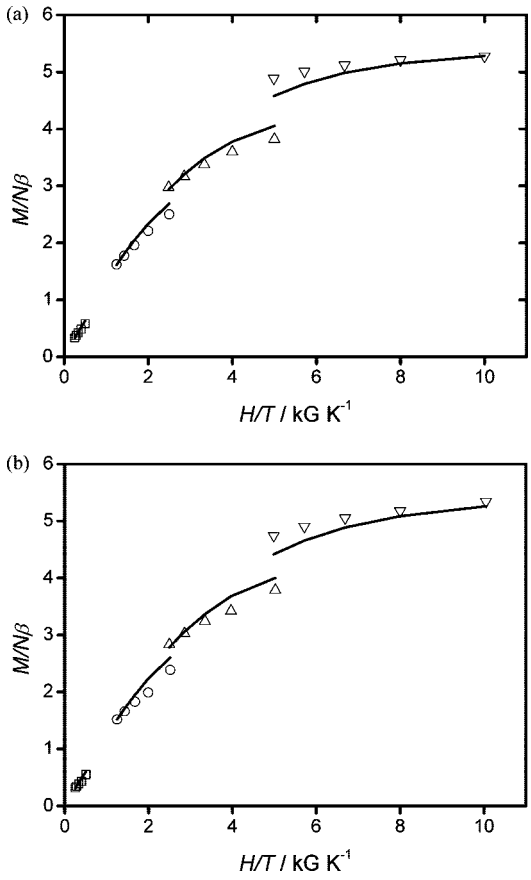

Figure 9. The reduced magnetization of (a) **3**·H_2O and (b) **4** plotted as $M/N\beta$ versus H/T at 1 (□), 5 (○), 10 (△), and 20 (▽) kG in eicosane.

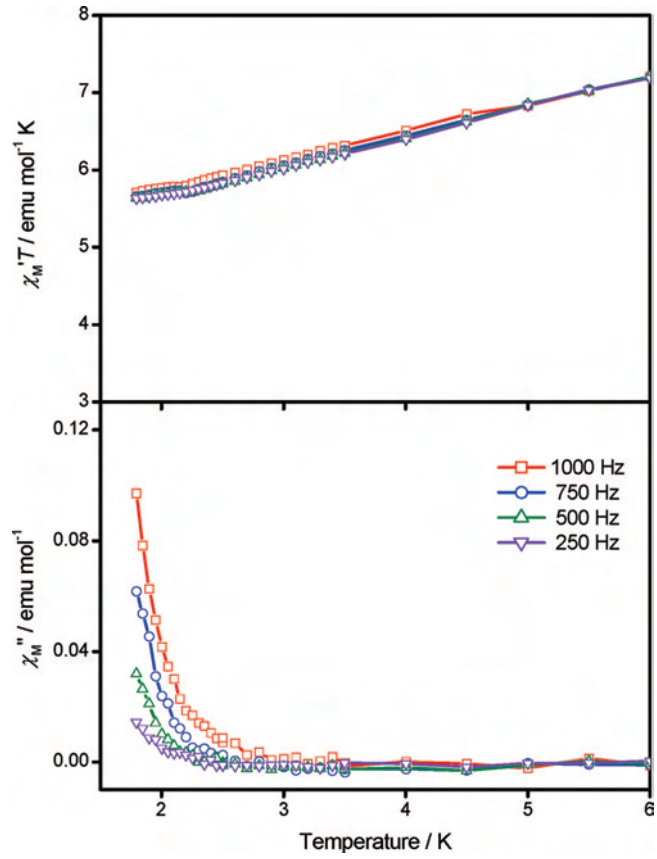

Figure 10. Plots of (top) $\chi_M'T$ and (bottom) χ_M'' vs temperature for a microcrystalline sample of complex **3**·H_2O in a 3.5 G AC field. The data were collected in an AC field oscillating at the indicated frequency.

1.04 cm^{-1} for these interactions in **1** and **2**, respectively, fall within this range. Since the low-lying excited state $S = 2$ of complexes **1** and **2** could be populated even at temperatures down to 1.8 K, the given results of fitting $S_T = 1$ from reduced magnetization measurements are not reasonable.

Magnetic Properties of Complexes 3 and 4. Solid-state, variable-temperature magnetic susceptibility measurements were performed on microcrystalline samples of complexes **3**·H_2O and **4**, all suspended in eicosane to prevent torquing. The DC magnetic susceptibility data were collected in the 2.0–300 K range in a 1.0 kG magnetic field. As can be seen in Figure 8, the magnetic behaviors of the two complexes are very similar. For **3**·H_2O, $\chi_M T$ steadily decreases with decreasing temperature from 16.61 emu mol^{-1} K at 300 K to 12.75 emu mol^{-1} K at 30 K, below which the $\chi_M T$ value decreases more rapidly to 5.91 emu mol^{-1} K at 2.0 K. Likewise for **4**, $\chi_M T$ gradually decreases from 16.93 emu mol^{-1} K at 300 K to 12.59 emu mol^{-1} K at 30 K. Below this temperature, $\chi_M T$ again decreases more rapidly to 5.96 emu mol^{-1} K at 2.0 K. The values of $\chi_M T$ for two Mn_6 complexes at 300 K are lower than that expected for a cluster of three Mn^{II} and three Mn^{III} noninteracting ions (22.12 emu mol^{-1} K for $g = 2$), suggesting that antiferromagnetic couplings dominate the overall intramolecular exchange interactions within the complexes. The observed rapid decrease of the $\chi_M T$ value for temperatures below 30 K is most likely because of the zero-field splitting effect and perhaps weak intermolecular interactions mediated by the π stacking observed for **3** in the crystal structure. Because of the topological complexity of the molecule, it is not possible to determine the individual pairwise Mn exchange interactions using the Kambe method.[51] To determine the spin of the ground state, magnetization (M) measurements were performed in the 2.0–4.0 K temperature range and the 1.0–20 kG DC magnetic field range. The data of complexes **3**·H_2O and **4** are plotted as the reduced magnetization ($M/N\beta$) versus H/T in Figure 9a and b, respectively, where N is Avogadro's number, β is the Bohr magneton, and H is the applied magnetic field. For a system occupying only the ground state and experiencing no ZFS, the various isofield lines would be superimposed and $M/(N\beta)$ would saturate at a value of gS. The nonsuperposition of the isofield lines in Figure 9 is indicative of the presence of significant zero-field splitting. The data were fitted using the ANISOFIT[52] program, assuming only the spin ground state of the molecule is significantly populated. The best fitting for complex **3**·H_2O was obtained with the following parameters: $S = {}^7/_2$, $g = 1.98$, $D = -0.56$ cm^{-1}, and $E = -0.04$ cm^{-1}; complex **4** was best fit to $S = {}^7/_2$, $g = 1.90$, $D = -0.46$ cm^{-1}, and $E = -0.003$ cm^{-1} (where D is the axial ZFS parameter and E is the rhombic ZFS parameter). The measurements of the AC magnetic susceptibility were performed on vacuum-dried, microcrystalline samples of complexes **3**·H_2O and **4** in the

(51) Kambe, K. J. *Phys. Soc. Jpn.* **1950**, *5*, 48.
(52) Shores, M. P.; Sokol, J. J.; Long, J. R. *J. Am. Chem. Soc.* **2002**, *124*, 2279.

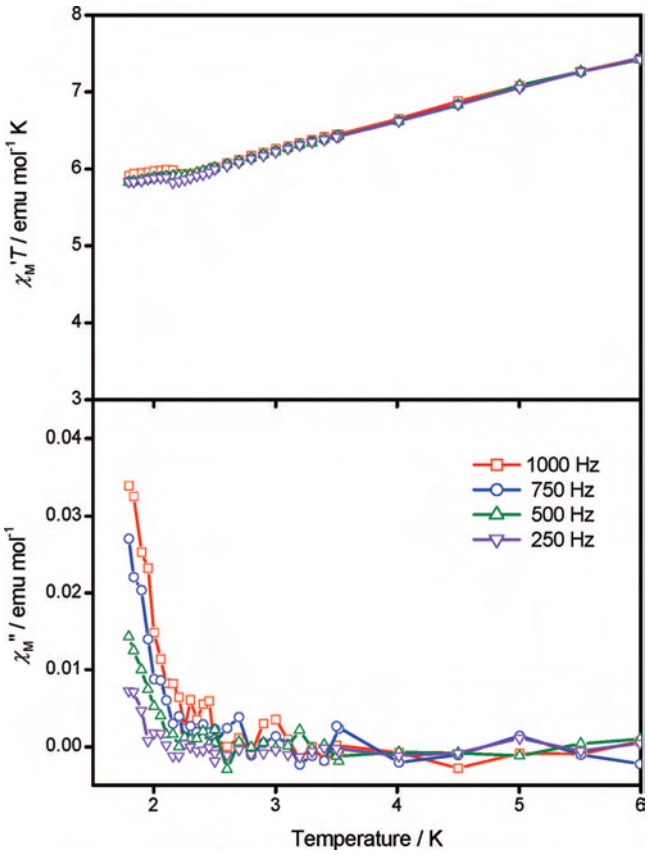

Figure 11. Plots of (top) $\chi_M'T$ and (bottom) χ_M'' vs temperature for a microcrystalline sample of complex **4** in a 3.5 G AC field. The data were collected in an AC field oscillating at the indicated frequency.

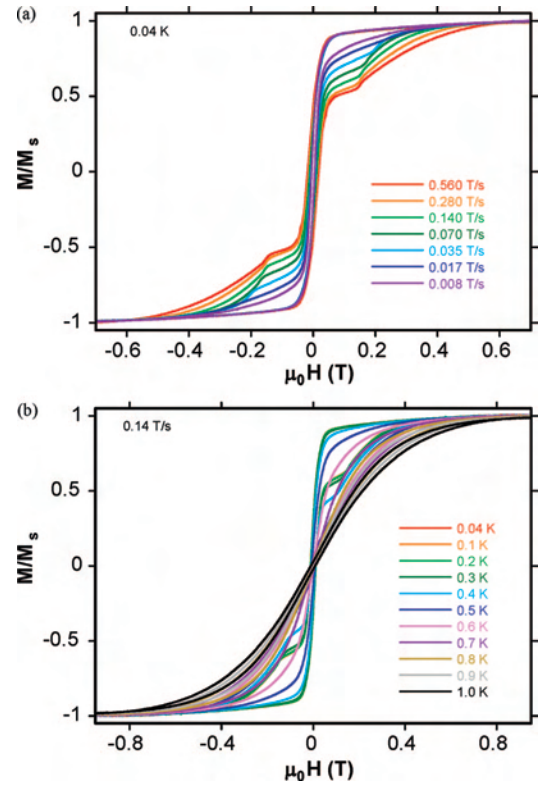

Figure 12. (a) Magnetization (M) vs applied magnetic field hysteresis loops for complex **3**·1.5CH_2Cl_2·Et_2O·H_2O in the 0.008–0.560 T/s sweep rate range at 0.04 K. (b) Magnetization (M) vs applied magnetic field hysteresis loops for **3**·1.5CH_2Cl_2·Et_2O·H_2O in the temperature range 0.04–1.0 K at a 0.14 T/s sweep rate. M is normalized to its saturation value, M_s.

temperature range 1.8–10 K in a zero DC field and a 3.5 G AC field oscillating at frequencies in the 250–1500 Hz range. The results for representative of complexes **3**·H_2O and **4** are shown in Figures 10 and 11, respectively. If the magnetization vector can relax fast enough to keep up with the oscillating field, there is no imaginary (out-of-phase) susceptibility signal (χ_M''), and the real (in-phase) susceptibility (χ_M') is equal to the DC susceptibility. However, if the barrier to magnetization relaxation is significant compared to thermal energy (kT), there is a nonzero χ_M'' signal and the in-phase signal decreases. In addition, the χ_M'' signals will be frequency-dependent. Such frequency-dependent χ_M'' signals are a characteristic signature of the superparamagnetic-like properties of a SMM (but by themselves do not prove the presence of a SMM). The sloping $\chi_M'T$ versus T plot is strongly indicative of a population of low-lying excited states since occupation of only the ground state would give an essentially temperature-independent value. At lower temperatures, the in-phase signal decreases and a frequency-dependent χ_M'' signal appears, which is suggestive of the slow relaxation of a single-molecule magnet. However, the peak maxima clearly lie at temperatures below 1.8 K, the operating limit of our instrument. The data thus suggest that complexes **3**·H_2O and **4** indeed exhibit the slow magnetization relaxation of SMMs.

Single-Crystal Hysteresis Studies. In order to confirm whether **3**·1.5CH_2Cl_2·Et_2O·H_2O is a SMM, magnetization versus applied DC field data down to 0.04 K were collected on a single crystal using a micro-SQUID apparatus.[53] Figure 12 shows the corresponding magnetization responses at 0.04∼1.0 K and a fixed field sweep rate of 0.14 T/s, as well as magnetization responses at 0.08∼0.56 T/s field sweep rates and a constant temperature of 0.04 K. Below 1.0 K, hysteresis loops are observed in the easy direction, and they become temperature-independent below 0.5 K, staying, however, field-sweep-rate-dependent even at 0.04 K, indicating that it occurs purely by a QTM. When these hysteresis loops are analyzed in more detail, two steps are observed due to a fast relaxation process at 0.04 K at $H = 0$ and 0.16 T. The large step at zero field corresponds to the fast ground-state QTM between the $Ms = \pm^7/_2$ states (corresponding to ∼75% reversal of the magnetization). Upon scanning the field to larger values, the second step is observed at about 0.16 T. If this step is QTM for the ground state ($Ms = -^7/_2$) to an excited state ($Ms = {}^5/_2$), the field separation will result in a value of $D/g \approx 0.15$ cm^{-1}. However, this value is mach smaller than the value obtained from fits of the magnetization data for **3**·H_2O ($D/g = -0.28$ cm^{-1}), and this step is not assumed as a QTM process from $Ms = -^7/_2$ to $Ms = {}^5/_2$, but a process of spin–spin cross-relaxation (SSCR).[54] The phenomenon of SSCR is the result of intermolecular exchange interactions, possibly through the π interaction

(53) Wernsdorfer, W. *Adv. Chem. Phys.* **2001**, *118*, 99.
(54) Wernsdorfer, W.; Bhaduri, S.; Tiron, R.; Hendrickson, D. N.; Christou, G. *Phys. Rev. Lett.* **2002**, *89*, 197201.

shown in Figure 5, and weak dipolar interactions between two (or more) SMMs.

In summary, hysteresis loops are seen in Figure 12, and their coercivities increase with increasing sweep rate and with decreasing temperature, as expected for the superparamagnet-like properties of a SMM. Hysteresis in magnetization versus field sweeps is the classical property of a magnet, and such loops are also a diagnostic feature of SMMs and superparamagnets below their blocking temperature (T_B). The data thus indicate that complex **3** is a new addition to the family of SMMs. The different structure-type SMMs comprised by Mn^{III}_6 are also reported in the literature.[43]

Concluding Comments. The pyridine-containing β-diketones (HL^1 and HL^2) have given proof for the new bridging ligands and have allowed the syntheses of four manganese compounds of different nuclearities and oxidation states. The reactions of HL^1 and HL^2 with $[Mn_3O(O_2CCl_3)_6(H_2O)_3]$ produce the two tetranuclear Mn clusters of complexes **1** and **2**, respectively, which contain a $[Mn^{II}_2Mn^{III}_2(\mu_4\text{-}O)]^{8+}$ core structure. The magnetic properties of **1** and **2** exhibit intramolecular antiferromagnetic exchange and possess an $S = 1$ ground state. In contrast, the parallel reactions between $[Mn_3O(O_2CPh)_6(H_2O)(py)_2]$ and HL^1 and HL^2 yield hexanuclear complexes **3** and **4**, respectively. Complexes **3** and **4** represent a new structural topology of $[Mn^{II}_3Mn^{III}_3(\mu_4\text{-}O)_2]^{11+}$ in the Mn chemistry. They have a ground-state spin value of $S = {}^7/_2$ that, together with a significant magnetoanisotropy, results in a small barrier to magnetization relaxation in AC susceptibility measurement and hysteresis loops at very low temperatures. Hence, complexes **3** and **4** are new members of the growing family of SMMs. The combined results demonstrate the ligating flexibility of the pyridine-containing β-diketone ligands, which are useful in the synthesis of mixed-valence manganese species.

Acknowledgment. The magnetic measurements were obtained from SQUID (MPMS XL-7) in NSYSU and we thank the National Science Council of Taiwan (NSC-95-2113-M-006-004) for financial support.

Supporting Information Available: X-ray crystallographic files in CIF format for complex $\mathbf{1}\cdot 2CH_2Cl_2$, $\mathbf{2}\cdot 2CH_2Cl_2\cdot H_2O$, $\mathbf{3}\cdot 1.5CH_2Cl_2\cdot Et_2O\cdot H_2O$ and $\mathbf{4}\cdot 3CH_2Cl_2$. This material is available free of charge via the Internet at http://pubs.acs.org.

IC7013368